A STUDY OF THE STOCHASTIC INSTABILITY OF THE BETATRON OSCILLATIONS OF AN ELECTRON BEAM IN A STORAGE RING

1973

BY

G.N. KULIPANOV, S.I. MISHNEV AND A.N. SKRINSKIĬ

Translated (November 1972) from the Russian *Izuchenie stokhasticheskoĭ neustoĭchivosti betatronnykh kolebaniĭ elektronnogo puchka v nakopitele.* Preprint No. 323, Institut yadernoĭ fiziki SOAN SSSR, Novosibirsk (1969), 51 pages.

TRANSLATED FOR
STANFORD LINEAR ACCELERATOR CENTER

A STUDY OF THE STOCHASTIC INSTABILITY OF THE BETATRON OSCILLATIONS OF AN ELECTRON BEAM IN A STORAGE RING

The authors undertake an experimental study of the behavior of the beam in an electron storage ring under the combined influence of two betatron-oscillation resonances and on periodic passage through a resonance.

They study conditions resulting in different types of particle motion. Depending on the experimental conditions, they observed: a) the existence of independent stable regions of phase stability; b) the appearance of second-order phase-stability regions and the formation of a stochastic layer near the boundary of the phase-stability region; c) a complete destruction of the phase-stability regions which imparts a stochastic character to the variation of the betatron-oscillation amplitudes.

The experimentally found conditions under which stochastic instability develops are compared with the theoretical findings of B.V. Chirikov. Experiments are described that prove the diffusional character of the particle motion in the stochastic region, as well as other experiments elucidating the character of the diffusion.

TABLE OF CONTENTS

Page

I. INTRODUCTION 1

II. EXPERIMENTAL SETUP AND EXPERIMENT SCHEMES 1

1. Storage-Ring Parameters 2

2. The System for Exciting Betatron-Oscillation Resonances 3

3. Ways of Measuring the Basic Parameters: Beam-Observation Methods 5

4. Selecting the Basic Parameters for the Conduct of the Experiments 6

III. STOCHASTIC BEAM INSTABILITY UNDER THE COMBINED EFFECT OF TWO BETATRON-OSCILLATION RESONANCES 8

1. Main Effects Observed with Excitation of a Single Resonance 9

2. Resonance Splitting - Formation of a Stochastic Layer in the Case of Two Resonances of Unlike Power 10

3. Complete Destruction of the Region of Phase Stability in the Interaction of Two Identical Resonances 14

IV. STOCHASTIC BEAM INSTABILITY DUE TO PERIODIC PASSAGE OF THE BETATRON OSCILLATIONS THROUGH A RESONANCE 16

1. Determining the Boundary of the Transition from a Slow ("Adiabatic") Crossing to the Stochastic Region 17

2. Measuring the Diffusion Coefficient in the Stochastic Region 19

3. Determining the Boundary of the Transition from the Stochastic Region to the Region of "Modulation" Resonances 22

4. Periodic Passage through a Resonance in the Presence of a Small Deviation 23

V. CONCLUSION 25

References 27

Figures 29

I. INTRODUCTION

The possibility of conducting experiments with proton-proton, and especially proton-antiproton, colliding beams is largely determined by whether the motion of the particles in the storage ring can be stabilized for a prolonged period, since various effects not observable in light-particle (e^- or e^+) storage rings can become appreciable through the absence of any natural damping mechanism. One of these effects is a stochastic instability of the betatron oscillations, possible under the combined action of several resonances or on periodic crossing through any resonance.[1]

The study of stochastic instability is not only of practical interest but also of theoretical interest, because it is here that we may find a transition from classical oscillation theory to statistical mechanics.[1]

Here we undertake an experimental study of the behavior of a beam in an electron storage ring under the simultaneous action of two betatron-oscillation resonances and on periodic passage through a resonance, and we ascertain the conditions under which a stochastic betatron-oscillation instability arises, and study the characteristics of the motion of the particles in that event. The experimental data are compared with the theoretical findings of B.V. Chirikov[1].

Since an electron beam in a storage ring is an ideal model of a nonlinear oscillator with very low friction[2], the experimental results obtained can be applied to other nonlinear systems too.

II. EXPERIMENTAL SETUP AND EXPERIMENT SCHEMES

The experiments were conducted in the BEP-1 electron storage ring.[3] The betatron-oscillation resonances (simultaneous radial and vertical, and also the sum resonance) were excited with the aid of an external resonant buildup

of the beam. This enabled us, for any values of the betatron-oscillation frequencies, to create one or another resonance, regulate the power of the resonances, and change the frequency distance between resonances, which cannot be done with the "machine" resonances excited by the imperfections of the guiding magnetic field at certain values of the betatron-oscillation frequencies. Moreover, using an external resonant buildup with frequency modulation made it technically simple to achieve periodic passage through a resonance, whereas the study of periodic passage through a "machine" resonance with the same parameters would have necessitated creating a complex system for modulation of the betatron-oscillation frequency.

1. Storage-Ring Parameters. For the experiments we used the upper storage track of the BEP-1 storage ring. Its parameters are: equilibrium radius R_i = 43 cm; working aperture A_z = ±1.0 cm, A_r = ±1.4 cm; revolution frequency f_o = 110.5 MHz; betatron-oscillation frequencies $f_z = \nu_z f_o$ = 85 MHz, $f_r = \nu_r f_o$ = 70.5 MHz. The cubic nonlinearity of the guiding magnetic field results in a dependence of the betatron-oscillation frequencies on the betatron-oscillation amplitude:

$$\frac{\partial \nu_z}{\partial a_z^2} = 7.7\times10^{-3}\,\frac{1}{\text{cm}^2} \qquad \frac{\partial \nu_z}{\partial a_r^2} = -1.5\times10^{-2}\,\frac{1}{\text{cm}^2}$$

$$\frac{\partial \nu_r}{\partial a_r^2} = 9.2\times10^{-3}\,\frac{1}{\text{cm}^2} \qquad \frac{\partial \nu_r}{\partial a_z^2} = -1.8\times10^{-2}\,\frac{1}{\text{cm}^2}\,.$$

Moreover, the betatron-oscillation frequencies depend also on the particle deflection from the equilibrium radius:

$$\frac{\partial \nu_z}{\partial r} = 3.5\times10^{-2}\,\frac{1}{\text{cm}} \qquad \frac{\partial \nu_r}{\partial r} = 4.2\times10^{-2}\,\frac{1}{\text{cm}}\,.$$

The stability of the betatron-oscillation frequency due to the ripple current in the storage-ring winding was usually $\frac{\Delta\nu}{\nu} \sim 6 \times 10^{-4}$, the ripple frequency 140 and 7 Hz. By using the lower track's magnet winding as a ballast load, and by connecting in parallel to the upper track a bank of capacitors with $C = 26$ mf and a storage battery with a capacity of 22.5 A/hr (the voltage across the cells being set equal to the voltage drop in the magnet winding), we succeeded in reducing the ripple ν to $\frac{\Delta\nu}{\nu} \sim 4 \times 10^{-5}$.

In addition to this spurious modulation of ν, there was always a "natural" modulation of the betatron-oscillation frequency due to the synchrotron oscillations and square-law nonlinearity. The synchrotron-oscillation frequency was usually $f_s = 3\text{-}5 \times 10^5$ Hz, the amplitude of the radial phase oscillations $a_{r\phi} = 0.3$ mm. With the existing quadratic nonlinearity, this gave us a frequency deviation $\Delta f_s = 10^5$ Hz.

2. *The System for Exciting Betatron-Oscillation Resonances.* To excite resonances in the storage-ring chamber, we set up a special system of electrodes which in the region of the beam produces a potential distribution:

$$V(X,Z) = \frac{V_1}{d}[x + \varepsilon_1 z] + \frac{V_2}{d^2}[x^2 - z^2 + 2\varepsilon_2 xz], \quad (1)$$

where V_1 and V_2 are the dipole and quadrupole terms of the expansion of the potential ($V_3 = V_4 = \ldots \approx 0$), and d is a characteristic geometric dimension. ε_k is the angle between the plane of symmetry of the k-th multipole and the plane $z = 0$.

If to these electrodes we apply the HF voltage $U = U_o \cos 2\pi f_p t$, then with the aid of this system we can excite resonances for any values of ν_r and ν_z by selecting, as required, the buildup frequency $f_p = \nu_p f_o$, since in this case the resonance condition is

$$m_r\nu_r + m_z\nu_z = n - \nu_p \qquad (2)$$

for $|m_r| + |m_z| \leq 2$, since $V_1 \neq 0$, $V_2 \neq 0$ while $V_3 = V_4 = \ldots = 0$. We usually used the following frequencies:

a) $f = f_o(1 - \nu_z)$ to excite the vertical betatron oscillations (Fig. 2a);

b) $f = f_o(1 - \nu_r)$ to excite the radial betatron oscillations (Fig. 2b);

c) $f = f_o(2 - \nu_r - \nu_z)$ to excite the sum resonance (Fig. 2c).

In addition to this system of electrodes inside the chamber, there were three pairs of flat plates creating a uniform field with respect to z. These plates were used for simultaneous excitation of several resonances of the vertical betatron oscillations at the frequency $f = f_o(1 - \nu_z)$.

The voltage for exciting the resonances was fed through power amplifiers from four master oscillators. The frequency of the oscillators was determined with the aid of a crystal-coated frequency meter. Moreover, the difference between the frequencies of two oscillators was measured with a special low-frequency frequency meter, with the aid of which the frequency distance between two resonances could be determined directly.

The master oscillators used allowed an external frequency modulation with the modulation frequency f_M = 0-60 kHz and deviation Δf_M = 0-200 kHz. The modulation frequency was set from an audio oscillator, and the deviation was determined with a deviation meter.

In some cases the buildup voltage was fed through a pulsed on-off switching unit operating as a key from the external trigger pulse. The transmission coefficient was 1:500 at f = 25 MHz, the voltage rise (decay) time $\tau \sim 10$ μs.

The system for exciting the resonances is shown schematically in Figure 1.

3. Ways of Measuring the Basic Parameters. Beam-Observation Methods. The simplest and most convenient methods of observing an electron beam in a storage ring are based on recording the synchrotron radiation (Fig. 1). A special optical system produced an image of the beam cross-section with a 2:1 magnification. Absolute calibration of the optical system's transfer constant was done with the aid of "aperture" probes placed in the storage-ring chamber on the beam-observation azimuth.

By observing the beam image near a resonance, we could determine the basic parameters of the region of betatron phase stability (RBPS):[2]

a) the equilibrium amplitude (a_0) from the visually observed beam image or from oscillograms obtained with the aid of a dissector[4];

b) the size of the RBPS from the dependence of the lifetime of the particles in the RBPS on the size of the beam in the RBPS; the beam size was increased with the aid of a system of nonresonant beam buildup[5] and was determined with the aid of a dissector;

c) the frequency of the small phase oscillations f_ϕ by resonant excitation of oscillations in the RBPS through modulation of the betatron-oscillation frequency ($\frac{\Delta\nu}{\nu} \sim 10^{-3}$); to modulate ν, a voltage from a standard audio oscillator on a frequency $f = f_\phi$ was fed through a ferrite-ring matching transformer to the ν-correcting plates; the increase in the oscillation amplitudes in the RBPS was observed with the dissector;

d) the particle distribution with respect to betatron-oscillation amplitudes from oscillograms obtained with the dissector; since the dissector's scanning frequency was $F = 25$ Hz, in the event of a fast change of position of the equilibrium amplitude of an RBPS with a frequency greater than F, we observed a stroboscopic picture from the dissector output (see Fig. 14d);

e) the particle distribution with respect to the betatron-oscillation

phases from the signal from a "fast" photomultiplier with a slit diaphragm; this photomultiplier made it possible to observe the coherent oscillations of a beam with a frequency of up to 30 MHz.

4. *Selecting the Basic Parameters for the Conduct of the Experiments.* The experimental study of the stochastic instability of the betatron oscillations in a storage ring was actually conducted against a background of various processes that affect the beam's behavior, processes therefore capable of blurring the effects being studied. Such processes are:

1) modulation of the betatron-oscillation frequency because of the synchrotron oscillations;

2) instability of the betatron-oscillation frequencies because of modulation of the current in the winding of the power supply of the storage-ring magnet;

3) scattering of the residual gas on atoms;

4) radiation damping.

Given our parameters ($\Delta f_s = 10^5$ Hz, $f_s = 5 \times 10^6$ Hz), the modulation of the betatron-oscillation frequency due to the synchrotron oscillations and quadratic nonlinearity produces a series of synchrobetatron resonances at a distance $\Delta f = nf_s$ (n = 1, 2, 3) from the main resonance.[2]

We were unable to study the stochastic instability of the synchrobetatron resonances because of the limited possibility of varying the distance between these resonances, which is determined by the synchrotron-oscillation frequency. Despite reducing the quadratic nonlinearity, we did not succeed in completely eliminating these resonances.

Actually there was also a modulation of the betatron-oscillation frequency due to the ripple current in the winding of the storage-ring magnet. This resulted in slightly altering the position of the equilibrium amplitude of the RBPS with a frequency of 140 and 7 Hz.

That is why the resonance power was selected so that the frequency of the phase oscillations in the RBPS would be much lower than the synchrotron-oscillation frequency (f_s) and much higher than the ripple frequency of the current in the magnet winding ($f_{ny\Lambda}$). Actually we were working with $0.1\ f_s > f_\phi > 50\ f_{ny\Lambda}$.

With $f_\phi \sim 0.1\ f_s$, the size of the RBPS with respect to the betatron-oscillation amplitudes was large enough to permit study of the oscillations within the RBPS itself. Since these oscillations are essentially nonlinear, we were able not only to excite forced oscillations of the particles in the RBPS due to the external resonant perturbation but to watch the formation of a second-order RBPS. We could not observe the formation of any higher-order RBPS, because the steady-state size of the beam was apparently greater than the sizes of those RBPS.

The natural beam dimensions are determined by the radiation-damping time and the magnitude of the diffusion due to scattering of the residual gas on atoms, and of the quantum fluctuations of the synchrotron radiation. Since under our conditions the vertical dimension was determined solely by the scattering of the residual gas on atoms,[6] and since for this process the diffusion coefficient Di decreases with increasing energy, the basic experiments were conducted with resonances of the vertical betatron oscillations at an energy E = 125 MeV.

The beam's vertical dimension at this energy ($2\ \delta_z \approx 0.1$ mm) determined the size of the natural stochastic region. The stochastic instability due to interaction of the resonances was observable only when it produced a diffusion coefficient greater than Di .

III. STOCHASTIC BEAM INSTABILITY UNDER THE COMBINED EFFECT OF TWO BETATRON-OSCILLATION RESONANCES

Many theoretical works[1,7,8] on the interaction of resonances in non-linear systems have recently appeared. However, the mathematical complexity of the problem has so far blocked construction of any rigorous theory, so that an experimental study of the matter may serve as a useful supplement to the existing theoretical endeavors.

We shall begin our experimental study with a very simple case of the interaction of two resonances. As the basic characteristics of the interaction we take the overlap parameter

$$s = \left|\frac{\Delta f}{f_{\phi 1}}\right|$$

and the parameter

$$m = \frac{f_{\phi 2}}{f_{\phi 1}},$$

which characterizes the power ratio of the interacting resonances. We recall that Δf is the frequency distance between the resonances, $f_{\phi 1}$ and $f_{\phi 2}$ the frequencies of the small phase oscillations in the RBPS, while $\Delta f_p = 4 f_\phi$ is the frequency width of the RBPS.

The studied resonance we shall call the first resonance ($RBPS_1$), and the second resonance ($RBPS_2$) will be a perturbation.

Depending on the values of s and m, with co-excitation of the two resonances we were able to observe:

1) the existence of two independent regions of phase stability (Fig. 3a and 3b);

2) a splitting of the resonances with the resulting appearance of new stable regions of phase stability inside the first two (Fig. 3c and 3d);

3) complete destruction of the region of betatron phase stability with a resulting stochastic character of the variation of betatron-oscillation

amplitudes (Fig. 3e and 3f).

For the reasons stated above, we studied in detail the one-dimensional case of the interaction of two resonances of the vertical betatron oscillations for different values of the parameters s and m. The entire range of variation of the parameter m can be divided (somewhat arbitrarily) into three characteristic regions, though of course there is no sharp boundary between one and another.

1. Main Effects Observed with Excitation of a Single Resonance (m = 0). The excitation of a single resonance has been studied in detail before.[2] Let us just remember that, owing to a peculiar phase-stability mechanism, a region of stable amplitudes and phases arises near the resonance, the region of betatron phase stability (RBPS). Of the particles that have entered this region, the amplitude and phase are subjected to a beat having the frequency of the phase oscillations (f_ϕ) and, owing to the radiation friction, decay to their equilibrium values. The scattering of the residual gas on atoms and the magnitude of the radiation damping determine the steady-state size of the beam in the RBPS (the size of the beam in the RBPS is not dependent on the power of the resonance and is equal to the size of the beam in equilibrium orbit without resonance excitation). The spread of the betatron-oscillation amplitudes and the resonance power determine the particles' betatron-oscillation phase spread. Hence the particles trapped in the RBPS constitute a coherent bunch having a relatively narrow spread of betatron-oscillation amplitudes and phases.

We should note that, depending on the buildup voltage and on the frequency separation with respect to the exact resonance, the existence of either one or two stable amplitudes is possible. Figure 5 shows photographs of the beam near the resonance for various frequency separations

$$\Delta f = f_o - f_{zo} - f_p ,$$

where f_o is the revolution frequency, f_{zo} the small-amplitude betatron-oscillation frequency, f_p the buildup frequency. The buildup voltage was constant ($U_{buildup}$ = 150 V). Figure 6 shows a resonance curve, the dependence of the amplitude on the frequency of the buildup voltage, plotted from such photographs. That same figure shows a skeleton curve plotted for a low build-up voltage ($U_{buildup}$ = 3 V).

The obtained resonance curve corresponds exactly to the theoretical concepts[9] of the resonance excitation of a nonlinear oscillator. This once more clearly shows that an electron beam in a storage ring is an ideal model of a nonlinear oscillator with very little friction.

For the experiments we used the excitation of resonances with both one and two equilibrium amplitudes. In the first case all the particles were trapped in one RBPS, and the lifetime of the particles in the RBPS equaled the lifetime of the beam in the absence of any resonance excitation. In the second case the lifetime of the particles in the RBPS, which was situated near the larger amplitude, was determined by the size of the RBPS and by the pressure of the residual gas[2] and, for our parameters, was usually $\tau \leq 50$ sec. A particle that slipped out of the RBPS was not completely lost, however, but damped to the small amplitudes.

2. *Resonance Splitting - Formation of a Stochastic Layer in the Case of Two Resonances of Unlike Power ($m < 0.6$).* The main effect observed with these values of m is the excitation of forced oscillations of the beam as a whole in $RBPS_1$ with a frequency of $f = \Delta f$. The presence of particle phasing in the RBPS in the case of a single resonance has the result that on this storage-ring azimuth the intensity of the synchrotron radiation from the beam varies with the frequency $f = nf_o - f_z$. We recorded this intensity

variation by using a photomultiplier with a slit diaphragm. The excitation of the forced oscillations of the beam in the RBPS registered through the modulation of the HF signal from the photomultiplier. We should note that in the case $s = 1$ and $s = 2$ the modulation amplitude was substantially greater than for other values of s. The excitation of the beam oscillations in the RBPS with $s = 1$ and $s = 2$ could also be seen from the density-distribution oscillograms (see Fig. 7).

Measuring the lifetime of the particles in the RBPS (see Fig. 8) proved a convenient way to study the characteristics of the interaction of the resonances for these values of m. For this, a disturbed resonance was excited so that there existed two stable amplitudes. We measured the lifetime of the particles in $RBPS_1$, which was situated near the larger amplitude. As seen from Figure 8, the dependence of the lifetime on s has a resonant character, and the lifetime in the RBPS decreased as $s = 4, 3, 2, 1, \frac{1}{2}, \frac{1}{3} \ldots$

All of these results are readily explainable if we consider that the presence of $RBPS_2$ is a nonlinear perturbation for the oscillations in $RBPS_1$, the frequency of the perturbation being $f = \Delta f$. Since the oscillations in $RBPS_1$ are also nonlinear, resonances with $\Delta f = \frac{p}{q} f_{\phi 1}$ (where p and q are integers) are possible in such a system. Accordingly, with $s = \frac{p}{q}$ a second-order RBPS can form inside $RBPS_1$. With values of $s = 1$ and $s = 2$ the second-order RBPS will be fairly large in size and observable from the particles' amplitude distribution (Fig. 7b). For other resonance values of s the second-order RBPS will show up only as an intermediate zone for particles emerging from the main RBPS owing to the scattering of the residual gas on atoms, as reflected by the curve for the lifetime (Fig. 8).

Apart from this main, purely dynamic effect (formation of a second-order RBPS), the interaction of the two resonances, given these m parameters,

will result in a partial destruction of the RBPS, i.e., in the formation of a stochastic layer near the separatriss, as theoretically predicted in refs. 1 and 7. The thinness of this layer, compared to the size of the second-order RBPS, makes it virtually impossible to discern its influence on the lifetime of the particles in the RBPS. We were enabled to observe such a layer only with the aid of the particles passing through the RBPS owing to the radiation damping, as was done by Dikanskiĭ et al.[10]

For this, we used one of the buildup systems, connected via a pulsed-switch unit, to create a resonance region ($RBPS_3$) in which all the beam's particles became trapped. By varying the buildup frequency, we gradually increased the equilibrium amplitude of $RBPS_3$ and switched the particles to the maximum amplitude. After this, two more resonance regions ($RBPS_1$ and $RBPS_2$) were created in the intermediate amplitude region for different powers and frequency distances between them. Then, with the aid of the pulsed-switch unit, the buildup voltage creating $RBPS_3$ was switched off, and the particles originally trapped in $RBPS_3$, owing to the radiation damping, decreased their amplitude and passed through the intermediate region. The instant at which the particles of amplitude $a = 0.5$ mm passed through was recorded with the aid of a slit-diaphragm photomultiplier. We also recorded the spread of the particles' betatron-oscillation amplitudes by measuring the time of the photomultiplier-pulse trailing edge.

As was shown experimentally in ref. 10, when particles pass through a single RBPS, the following effects are observed:

1) The particles become trapped in the RBPS, the capture probability being

$$W_c = \frac{|J_c|}{|J_c| + |J_1|},$$

where $|J_c|$ is the phase volume of the RBPS, $|J_1|$ the phase volume of the small-amplitude region lying inside the RBPS.[8]

2) The damping time of the uncaptured particles decreases owing to the fact that, in passing through the RBPS, the particles abruptly decrease the betatron-oscillation amplitude to the width of the RBPS, $2\Delta\alpha$ (the "phase-shift" effect in the betatron phase space).

3) The spread of the uncaptured particles' betatron-oscillation amplitudes increases because of the betatron-oscillation amplitude beats in the region inside the RBPS (we should note, though, that the arrival time of the very last particles was no later than τ_{z_1}, the normal damping time of the particles with the RBPS switched off).

The passage of the particles through the region of interaction of the two resonances $RBPS_1$ and $RBPS_2$ had the result that:

a) The entrapment of particles in $RBPS_1$ decreased. The dependence of the capture probability on the parameters s and m is shown in Figure 9.

b) There appeared on the oscillograms a long exponential "tail" corresponding to particles whose arrival times were several times longer than τ_{z_1}. The dependence of τ_z on the parameters s and m is shown in Fig. 10.

It is these results that do seem to indicate that, in addition to the purely dynamic effects (formation of a second-order RBPS), the interaction of the resonances in the $m < 0.6$ region, even in the absence of any diffusion at the RBPS center, results in a decrease of the RBPS width due to the stochastic layer that forms near the separatriss. The decrease of the RBPS width is evident from the decreased capture of particles (Fig. 9). That this decrease of the RBPS width indeed is linked to the stochastic layer is evident from the simultaneous increase of τ_z for the uncaptured particles (Fig. 10). Such an increase of the damping time characterizes particles which diffuse for a time in the stochastic layer, then emerge into the small-amplitude region, where they undergo normal radiation damping.

These results can be interpreted also as a manifestation of a particle-heating mechanism in a certain amplitude region. An analogous result would be obtained if the particles were to pass through a thin gas target instead of a region of interaction of two RBPS.

3. Complete Destruction of the Region of Phase Stability in the Interaction of Two Identical Resonances ($m \sim 1$). In this range of variation of the parameter m the main observable effects are the diffuse "spreading" of the beam in the amplitude region determined by the size of $RBPS_1$, and complete destruction of the RBPS.

The destruction of the RBPS can be inferred, first of all, from the sharp drop in the HF signal from the diaphragmed photomultiplier. With s = 0.2-1.2 and s = 2 the photomultiplier recorded only the noise signal, which indicates a uniform distribution of the particles with respect to betatron-oscillation phases, and a complete absence of the phase-stability mechanism.

In Figure 4, which shows photographs of the beam, we see that for s = 1 and s = 2 the particles are almost evenly distributed with respect to amplitudes too in the amplitude region determined by the size of $RBPS_1$. With s = 3 we observed a large diffuse increase in the size of the beam in the RBPS, but the amplitude distribution still had its maximum at $a \approx a_0$ (a_0 being the equilibrium amplitude of the RBPS). With s = 1.5 and s = 2.5 only the formation of the second-order RBPS was observed.

A variation of the particle distribution with respect to betatron-oscillation amplitudes could be observed only in the case of excitation of a disturbed resonance ($RBPS_1$) with one stable amplitude. But if the disturbed resonance was excited with two stable amplitudes, then the switching-on of $RBPS_2$ when m > 0.6 caused the particles quickly to leave the RBPS near the large amplitude and damp into the small-amplitude region. In this case we

found it convenient to observe the decrease of the electron density in $RBPS_1$ after $RBPS_2$ was quickly switched on. The density decrease was recorded with the aid of a photomultiplier whose diaphragm was tuned to the center of $RBPS_1$. The density decrease was exponential in character (see Fig. 11). The dependence of the time constant on the parameters s and m is shown in Figures 11a and 11b. Characteristically the dependence on s is of a resonance nature.

For a more complete understanding of how the character of the motion of an individual particle changes as we go from $m = 0$ to $m = 1$ $(s = 2)$, we ran a special experiment. After switching on the first resonance, we quickly switched on $RBPS_2$ and, with the aid of a diaphragmed photomultiplier, watched the particles pass from $RBPS_1$ to $RBPS_2$. The slit diaphragm was tuned to $RBPS_2$ so that initially there was no signal from the photomultiplier.

Since initially the particles in the RBPS are phased, by observing the guidance of the entire beam for a length of time shorter than that required for loss of coherence, we can infer the nature of the motion of one particle. Figure 12 shows oscillograms of the photomultiplier current, from which we see that the particles' amplitude variation is jerky, and the amplitude may either decrease or increase. The characteristic times of the amplitude variation are much longer than the betatron-oscillation period but shorter than the phase-oscillation period in the RBPS.

Summarizing all the experimental results obtained over a broad range of variation of the parameters s and m, we are able to conclude that:

1) The interaction of the two resonances essentially manifests itself only in the case of the resonance overlap $s = \left|\frac{\Delta f}{f_\phi}\right| < 4$.

2) The main consequence of the resonance interaction is a splitting of the resonances, the formation of a second-order RBPS at certain values of $s = \frac{p}{q}$.

3) The resonance splitting is always accompanied by formation of a stochastic layer near the separatriss.

4) Complete stochastic destruction of the RBPS is observed only for certain values of s and m, which clearly confirms the fact that the phase-stability region is destroyed precisely because of an overlapping of the second-order RBPS, which form at certain values of s and which apparently overlap only when $m \approx 1$.

IV. STOCHASTIC BEAM INSTABILITY DUE TO PERIODIC PASSAGE OF THE BETATRON OSCILLATIONS THROUGH A RESONANCE

The question of periodic passage through a resonance has long been of interest to many investigators. We should note, however, that even until very recently there were no clear answers to the following: Where lies the boundary between a slow and a fast passage? What exactly is the transition region? How do we allow for the amplitude increments in the case of a fast passage? And so forth. Even after publication of B. Chirikov's paper[11], in which the problem of periodic passage through a resonance was considered theoretically in its most general form, a number of works appeared, of which some were utterly incorrect[12], while others dealt only with certain special cases but without substantiating the limits of their analysis[13,14]. This situation may be due in part to the absence of any experimental work.

That is why we ran a series of experiments to study the periodic passage through a resonance under the most varied conditions. To some extent these experiments are a continuation of the experiments aimed at studying the interaction of two resonances, since the periodic passage through a resonance can be regarded as an interaction among a large number of resonances.

For the experiments we selected the resonance of the vertical beta-

tron oscillations that is excited by the resonant buildup of the beam. The resonance was usually excited with one stable amplitude (Fig. 14b). The periodic crossing was accomplished by introducing a frequency modulation of the buildup voltage. We measured the parameters: a_o and f_ϕ, the equilibrium amplitude of the RBPS and the frequency of the small phase oscillations in the RBPS in the absence of frequency modulation; f_M the modulation frequency; Δf_M the modulation depth (deviation).

Depending on how Δf_M, f_M and f_ϕ were interrelated, the periodic crossing of the resonance produced the following effects:

a) periodic variation of the position of the equilibrium amplitude (the size of the beam underwent virtually no change)["adiabatic" crossing];

b) diffuse blowup of the beam in a certain amplitude region [stochastic instability];

c) appearance of new stable regions, "modulation" resonances (analogue of the synchrobetatron resonances).

We should note that no sharp boundary is encountered on passing from one region into another. By utilizing certain characteristic transition regions, however, (concerning which, see below) we can assume an arbitrary boundary. Let us look more closely at the regions depicted in Figure 13 and at the boundaries between them, and let us distinguish in particular the small-deviation region, in which a periodic alternation of stable and unstable regions was observed.

1. Determining the Boundary of the Transition from a Slow ("Adiabatic") Crossing to the Stochastic Region. As shown in ref. 1, any crossing, no matter how slow, through a resonance results in destruction of the phase-stability region and in the formation of a stochastic layer in the region of the separatriss. The relative thickness of this stochastic layer

is

$$\delta \sim \frac{\Delta f_M f_M}{f_\phi^2} . \qquad (3)$$

That is why no slow crossing through a resonance, no matter how slow, can be called adiabatic. For the same reason Chirikov[1] asserts that there is no stochastic-instability boundary with a slow crossing.

However, we can introduce the concept of a lower bound of the complete destruction of the phase-stability region, i.e., when

$$\delta \sim 1 \quad \text{and} \quad \frac{f_\phi^2}{\Delta f_M f_M} \sim 1 . \qquad (4)$$

The introduction of such a boundary is the more appropriate as a boundary or limit of the complete destruction of the RBPS is readily observable experimentally.

Figure 14 shows oscillograms of the beam-density distribution obtained for a constant resonance power (f_ϕ = const) and deviation (Δf_M = const), and varying modulation frequency f_M. From these oscillograms we see that for small f_M (see Fig. 14c and 14d) the beam as a whole moves over into the amplitude range Δa_o. According to the measurements

$$\Delta a_o^2 = \frac{\Delta f_M}{f_o - \partial\nu/\partial a^2} .$$

This means that the thickness of the stochastic layer is small, the size of the undestroyed RBPS is large compared to the dimensions of the beam in the RBPS, and that all the particles remain trapped in the RBPS. As the modulation frequency is increased, the thickness of the stochastic layer increases, the size of the RBPS decreases, and particles not trapped in the RBPS appear, which "spread out" over the Δa_o amplitude range (see Fig. 14e). As the modulation frequency increases, the proportion of trapped particles decreases (see Fig. 14e) until finally all the particles become diffusely spread out

(see Fig. 14f), which indicates complete destruction of the RBPS.

The extent of the destruction of the RBPS could be determined with the aid of a slit-diaphragm photomultiplier, whose slit was tuned to the amplitude $a = a_0$. By measuring the ratio of the variable to the constant component of the photomultiplier current, we were able to find the ratio of the number of particles trapped in the RBPS to those spread out over the Δa_0 amplitude range. The boundary of the complete destruction of the RBPS was determined from the disappearance of the photomultiplier current's variable component (see Fig. 15).

Figure 16 shows the dependence of the photomultiplier current's variable component on the modulation frequency for various values of Δf_M. We see that for small Δf_M either there is no complete destruction at all of the RBPS, only individual bands of its partial destruction being observable, or the boundary of its complete destruction has an oscillating character. The boundary of the complete destruction of the RBPS is determined with sufficient clarity only for $\Delta f_M > f_\phi$. For this region we plotted curves of the complete destruction of the RBPS as a function of the deviation (Fig. 17a) and resonance power (Fig. 17b). We found that for the case $\Delta f > f_M$ formula (4) qualitatively very well defines the boundary of complete destruction of the RBPS. The experimentally measured complete-destruction boundary corresponds to

$$\frac{f_\phi^2}{f_M \cdot \Delta f_M} \approx 4 . \qquad (5)$$

2. *Measuring the Diffusion Coefficient in the Stochastic Region.* In addition to the diffuse amplitude blowup of the beam with increasing modulation frequency, we observed at the same time a decrease of the signal, on the frequency $f = f_0 - f_z$, from the diaphragmed photomultiplier. In the case

$$\frac{f_\phi^2}{f_M \cdot \Delta f_M} < 4$$

the HF signal faded out entirely, which indicates the absence of any phasing of the particles and complete destruction of the RBPS. The character of the variation of the betatron-oscillation amplitudes became stochastic. Direct measurement of the diffusion coefficient afforded proof of this.

The diffusion coefficient D, which characterizes the rate of variation of the square of the betatron-oscillation amplitude,

$$D = \frac{[\Delta(a^2)]}{t}, \tag{6}$$

is a basic characteristic of the stochastic-instability region. In periodic passage through a resonance whose power is $B(a^2)$, when $\Delta f >> f_M$ the diffusion coefficient is written as[1]

$$D = \frac{\pi B^2(a^2) f_0^2}{\Delta f_M}. \tag{7}$$

The presence of diffusion and of radiation damping must lead to establishment of an equilibrium size $\overline{\Delta a}$. Taking into account (6), (7) and (from ref. 8)

$$f_\phi^2 = B f_0^2 \frac{\partial \nu}{\partial a^2}, \tag{8}$$

we get

$$\overline{\Delta a} = \frac{f_\phi^2}{2 a_0 f_0 \frac{\partial \nu}{\partial a^2}} \sqrt{\frac{\pi \tau_z}{\Delta f_M}}, \tag{9}$$

where f_ϕ is the frequency of the small phase oscillations in the RBPS situated near the equilibrium amplitude a_0, and τ_z is the vertical-betatron-oscillation damping time. Expression (9) is convenient for experimental verification, since it contains all the directly measured quantities.

Figure 18 shows oscillograms of the beam-density distribution in

the stochastic region for different values of the resonance power (Δf = const, f_M = const). From these oscillograms we see that for low resonance power and high Δf_M the beam-density distribution is close to a normal distribution. For high resonance power and low Δf_M the distribution differs from a normal distribution, the large amplitudes getting chopped off, so that the particles can have amplitudes no greater than

$$a_M = \sqrt{\frac{\Delta f_M}{f_o \cdot \partial\nu/\partial a^2}} ,$$

which indicates that diffusion is possible only in a certain amplitude region determined by the frequency deviation.

The presence of a sharp boundary between a stochastic region with a high diffusion coefficient and a region in which the diffusion is governed solely by the scattering of the residual gas on atoms can be inferred also from the dependence of the beam lifetime on the aperture (see Fig. 19). Fig. 19 shows two curves for a beam having one and the same size at the distribution-function half-height, but in the one case the increase of the beam size was achieved through a nonresonant beam buildup[5] giving a normal amplitude distribution, while in the other the beam-size increase was achieved through stochastic instability.

Characteristic in this sense is Figure 20, which gives the beam size as a function of the buildup frequency separation Δf with respect to the exact resonance (the buildup voltage, modulation frequency and deviation remained constant). Figure 20 makes very clear that the region of stochastic instability in the periodic passage through a resonance is strictly limited by the deviation. From that figure we also see that the beam size increases when $\Delta f = \Delta f_M$. This increase is apparently due to the fact that the points $\pm\Delta f_M$ are the points of slowest passage through the resonance, so that the time that the particles spend in the resonance increases, as does the diffusion

coefficient, which results in the increase in the size of the beam.

The diffusion coefficient and its dependence on the different parameters were measured by measuring the beam size in that region of the resonance power, Δf_M and Δf (see Fig. 18), in which the distribution does not differ from a normal distribution, and in which expression (9) holds.

Figure 21a shows the dependence of the beam size on f_ϕ^2 for two values of Δf_M. Figure 21b shows the dependence of the beam size on the deviation Δf_M. The beam size was not dependent on the modulation frequency when $\Delta f_M \gtrsim 20\ f_M$.

Qualitatively, all these measurements show that

$$\overline{\Delta a} \sim \frac{f_\phi^2}{\Delta f_M^{1/2}}.$$

Quantitative estimates were made for the following parameters: $f_\phi = 6.5 \times 10^3$ Hz; $a_o = 0.2$ cm; $\frac{\partial f_z}{\partial a_z^2} = 8.5 \times 10^5$ Hz/cm^2; $\Delta f_M = 10^5$ Hz. Calculation per formula (9) gives us $\overline{\Delta a}_{cal} = 1.8$ mm. Measurements of the beam size for these parameters (see Fig. 21) showed that $\overline{\Delta a}_{meas} = 1.45$ mm. We can therefore conclude that both qualitatively and quantitatively the experiment agrees well with the theoretical predictions.

3. *Determining the Boundary of the Transition from the Stochastic Region to the Region of "Modulation" Resonances.* On the basis of oscillograms of the electron beam's density distribution (see Fig. 14) obtained with a high modulation frequency, we can speak of the development of new stable regions of phase stability, or "modulation" resonances. The development of these resonances is a consequence of the frequency modulation of the exciting force, which can be expanded into a Fourier series:

$$F = F_0 \sum_{n=0}^{\infty} J_n\left(\frac{\Delta f_M}{f_M}\right) \cos 2\pi (f \pm n f_M) t, \qquad (10)$$

where $J_n(\frac{\Delta f_M}{f_M})$ is a Bessel function of the first kind of order n. From this we see that, in addition to the main resonance, we get a series of supplementary "modulation" resonances at a distance $\Delta f = \pm nf_M$ from the main one, the power of these resonances being $B_n \sim J_n(\frac{\Delta f_M}{f_M})$. When $\Delta f_M >> f_M$, the power of all the resonances is roughly the same, namely:[1]

$$B_n \approx B_o(\frac{f_M}{\Delta f_M})^{1/2}, \tag{11}$$

where B_o is the resonance power without the frequency modulation.

The condition of transition from the region of "modulation" resonances to the stochastic region[1] means physically an overlapping of the regions of phase stability of the "modulation" resonances and is written as

$$S = \frac{f_M}{f_{\phi M}} \sim 1, \tag{12}$$

where $f_{\phi M}^2 = B_n f_o^2 \frac{\partial \nu}{\partial a^2}$ is the frequency of the small phase oscillations in the RBPS of the "modulation" resonance. When allowance is made for (8) and (11), the stochasticity condition is written as

$$S = \frac{f_M^{3/4} \Delta f_M^{1/4}}{f_\phi} \sim 1. \tag{13}$$

The upper bound of the stochasticity was determined experimentally by measuring the electron-density distribution (see Fig. 14). Figure 22 shows the position of the boundary as a function of the resonance power for a constant deviation. The dependence of the boundary position on the deviation is shown in Figure 13. Good qualitative agreement with formula (13) is obtained only when $\Delta f_M > 2f_\phi$. In this region the experimentally measured boundary corresponds to

$$S = \frac{f_M^{3/4} \Delta f_M^{1/4}}{f_\phi} \simeq 1{,}85. \tag{14}$$

4. Periodic Passage through a Resonance in the Presence of a Small Deviation. The region of small deviations is of interest, and we shall discuss it separately, because here Chirikov's results[1] have limited

applicability, and because it is here that we see the transition from the old classical results (from, say, the problem of the stability of the solutions of equations with periodic coefficients) to Chirikov's findings[1].

Determination of the boundary of complete destruction of the RBPS in the presence of small deviations Δf_M has shown that in certain modulation-frequency regions a partial or complete destruction of the RBPS is observed even in the case $\frac{f_\phi}{f_M \Delta f_M} < 4$ (see Fig. 16). The relative extent of this destruction can be inferred from Figure 16, while Figure 13 shows the width of these modulation-frequency regions as a function of the deviation. The resonance power remained constant, and the frequency of the small phase oscillations f_ϕ was 36 kHz.

Figure 13 is strongly reminiscent of the stability diagram for the solutions of the Mathieu equation[15], since the regions of destruction of the RBPS lie near the modulation frequencies $2f_1$, f_1, $\frac{2}{3}f_1$, $\frac{1}{2}f_1$, $\frac{2}{5}f_1$, $\frac{1}{3}f_1$, ..., where $f_1 = 30$ kHz when $f_\phi = 36$ kHz.

The destruction of the RBPS at these values of the modulation frequency is apparently due to an interaction of the second-order phase-stability regions that form as a result of excitation of a parametric or subharmonic resonance in the RBPS. Excitation of these resonances is possible because the frequency modulation of the buildup voltage produces two effects: 1) a change in the position of the equilibrium amplitude of the RBPS, hence excitation of resonances in the RBPS when $f_M = \frac{f_\phi}{n}$; 2) modulation of the frequency of the phase oscillations in the RBPS, hence excitation of parametric resonances in the RBPS when $f_M = \frac{2f_\phi}{n}$ ($n = 1, 2, \ldots$). Since in the case of resonance at $f_M = \frac{f_\phi}{n}$ a parametric resonance is excited independently, this results in an amplification of these resonance bands. The fact that the regions of destruction of the RBPS lie not near the frequencies

$f_M = \frac{2f_\phi}{n}$ but near $f_M = \frac{2f_1}{n}$ (where $f_1 = 0.82\ f_\phi$) is apparently due to the substantial nonlinearity of the oscillations in the RBPS. The relation $f_1 = 0.82\ f_\phi$ held under variation of f_ϕ from 5 to 50 kHz.

The absence of a resonance structure in the case of large deviations is attributed, on the one hand, to the experimental difficulties in distinguishing the narrow resonance bands of high order and, on the other, to the overlapping of individual lower-order resonance bands. It is the overlapping of the resonance zones that gives us the stochastic region (Fig. 13).

V. CONCLUSION

The quite unique characteristics of an electron beam in a storage ring (long lifetime, little damping, small nonlinearity of the oscillations, simplicity of the observation methods) have made it possible to set up a number of "genuine" experiments for studying the characteristics of a nonlinear oscillator, and to conduct an experimental study of interesting physical problems formerly approachable only through mathematical experiments involving numerical solution of the equations of motion on an electronic computer[1].

In the present study we investigated the interaction of two resonances and the periodic passage through a single resonance in a nonlinear system. The interaction of two resonances is a very simple case of resonance interaction, whereas the periodic passage through a resonance is a more general case, since it can be regarded as the interaction of a large number of "modulation" resonances.

The most interesting experimental results can be considered to be:

1) We have demonstrated the possibility of a stochastic motion of particles under the influence of purely periodic perturbations. Our measurement of the diffusion coefficient in the stochastic region during periodic passage

through resonance, and our discovery of a heating of the particles in the stochastic layer in the interaction of two resonances, afford surprising experimental confirmation of this fact.

True, we must emphasize that the stochasticity of course does not signify the disappearance of the betatron oscillations. The stochastic instability results only in imparting to the variation of the betatron-oscillation amplitudes a random diffusional character. The characteristic period of this process is much longer than the betatron-oscillation period but shorter than the period of the phase oscillations in the RBPS.

2) We determined the conditions under which stochasticity arises. We have shown that the development of stochastic instability proceeds through purely dynamic effects: resonance splitting and formation of second-order RBPS. The overlapping of second-order RBPS results in stochastic destruction of the phase-stability region. This is why the stochastic instability observed in the interaction of two resonances and on periodic passage through resonance develops under certain resonance relationships.

3) We compared some of the experimental data with Chirikov's theoretical findings[1], and found a fairly good qualitative and quantitative agreement. In a number of cases we were able to write the numerical coefficients in Chirikov's formulae[1], the latter proving correct only in order of magnitude.

In addition, our experimental study yielded a few results of some practical value:

a) We demonstrated experimentally the possibility of creating a spatially sharply limited diffusion region with a recordable diffusion coefficient, which can be used, for example, to increase the size of the beam in an electron storage ring (which has been found necessary to suppress the collision effects in all operating storage rings). The possibility of obtaining an almost uni-

form density over the beam cross-section, and the absence of "tails" in the beam's amplitude distribution, enable one, with the aid of the stochastic buildup, to increase the size of the beam up to the half-aperture of the storage-ring chamber without shortening the lifetime through multiple processes.

b) We demonstrated experimentally the possibility of limiting the stochastic region of the betatron-oscillation amplitudes by reducing any stray frequency modulations and by introducing a large constant component of cubic nonlinearity.

c) Experimental determination of the numerical coefficients enabled us confidently to make quantitative estimates of the different effects for heavy-particle storage rings.

In conclusion the authors wish to express their profound gratitude to B.V. Chirikov, whose continuous advice on many points helped to make this study possible, and to N.S. Dikanskiĭ, S.G. Popov and G.M. Tumaĭkin for numerous useful discussions, to B.A. Lazarenko for creating the electronic apparatus, and to A.M. Chabanov for his assistance in conducting the experiments.

REFERENCES

1) B.V. Chirikov: *Issledovaniya po teorii nelineĭnogo rezonansa i stokhastichnosti* (Studies on the Theory of Nonlinear Resonance and Stochasticity). Dissertation, Novosibirsk (1969).

2) G.N. Kulipanov, S.I. Mishnev et al.: *Vliyanie nelineĭnosteĭ na betatronnye kolebaniya v nakopitele* (Influence of Nonlinearities on the Betatron Oscillations in a Storage Ring). Trudy Vsesoyuznogo soveshchaniya po uskoritelyam (Proceedings of the All-Union Conference on Accelerators), Moscow (1968). IYaF Preprint No. 251 (1968), Novosibirsk.

3) G.I. Budker, A.A. Naumov et al.: Proceedings of the International Conference on Accelerators, Dubna (1963), p. 275.

4) E.I. Zinin: Proceedings of the All-Union Conference on Accelerators, Moscow (1968).

5) E.I. Zinin et al.: Atomnaya energiya, No. 3 (1966), p. 220.

6) V.L. Auslender et al.: Atomnaya energiya, vol. 22 (1967), p. 200.

7) G.M. Zaslavskiĭ and N.N. Filonenko: ZhETF, vol. 54 (1968), p. 1599.

8) Ya.S. Derbenev: Dissertation, Novosibirsk (1968).

9) N.N. Bogolyubov and Yu.A. Mitropol'skiĭ: *Asimptoticheskie metody v teorii nelineĭnykh kolebaniĭ* (Asymptotic Methods in the Theory of Nonlinear Oscillations). 1967.

10) N.S. Dikanskiĭ et al.: *Izuchenie prokhozhdeniya chastits cherez oblast' avtofazirovki betatronnykh kolebaniĭ za schët radiatsionnogo zatukhaniya* (Study of the Passage of Particles through a Region of Betatron-Oscillation Phase Stability due to Radiation Damping). Report presented at the International Conference on Accelerators, Yerevan (1969).

11) B.V. Chirikov: Atomnaya energiya, vol. 6 (1959), p. 630.

12) V.I. Kotov et al.: Proceedings of the International Conference on Accelerators, Dubna (1963), p. 844.

13) P. Zenkevich: PTE, No. 1 (1967), p. 24.

14) A.A. Kolomenskiĭ: Atomnaya energiya, No. 6 (1965), p. 636.

15) Mak-Lakhlan: *Teoriya i prilozheniya funktsiĭ Mat'e* (Theory and Applications of Mathieu Functions), Moscow (1953). [Translator's Note: probably a translation from English; wording of original untitle uncertain; English spelling of author's name possibly McLaughlin.]

TRANSLATED FROM THE RUSSIAN BY

addis TRANSLATIONS International
post office box 4097
woodside, california 94062
(415) 851-1040

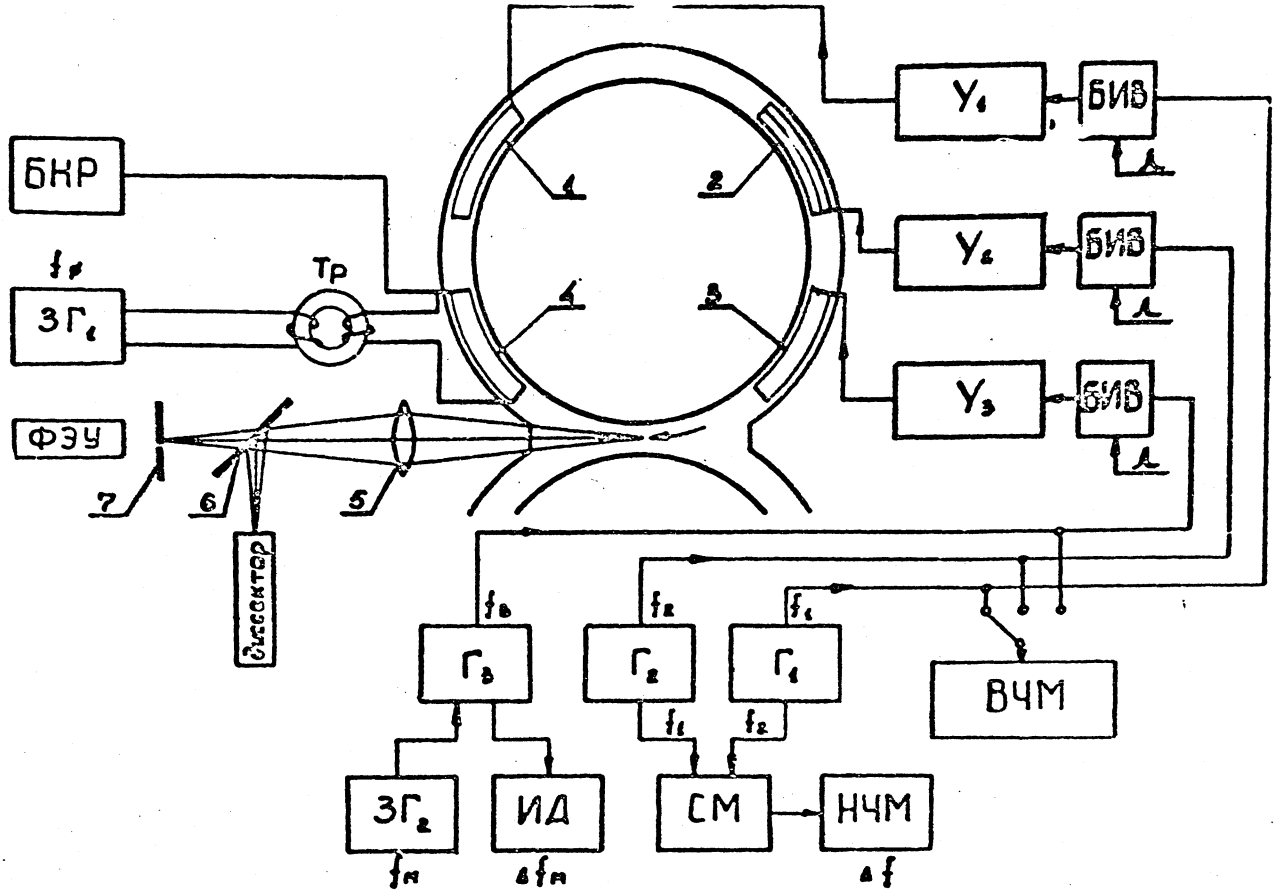

FIGURE 1: Diagram of the optical system of the BEP-1 storage ring and resonance-excitation system: 1, 3, 4 - buildup plates; 2 - buildup electrodes; 5 - lens; 6 - semitransparent mirror; 7 - diaphragm; Б Н Р - nonresonant-buildup unit; З Γ_{1-2} - audio oscillator; Γ_{1-3} - HF oscillator; $У_{1-3}$ - power amplifier; Б И В - pulsed on-off switching unit; В Ч М - HF frequency meter; Н Ч М - LF frequency meter; С М - mixer; И Д - deviation meter.

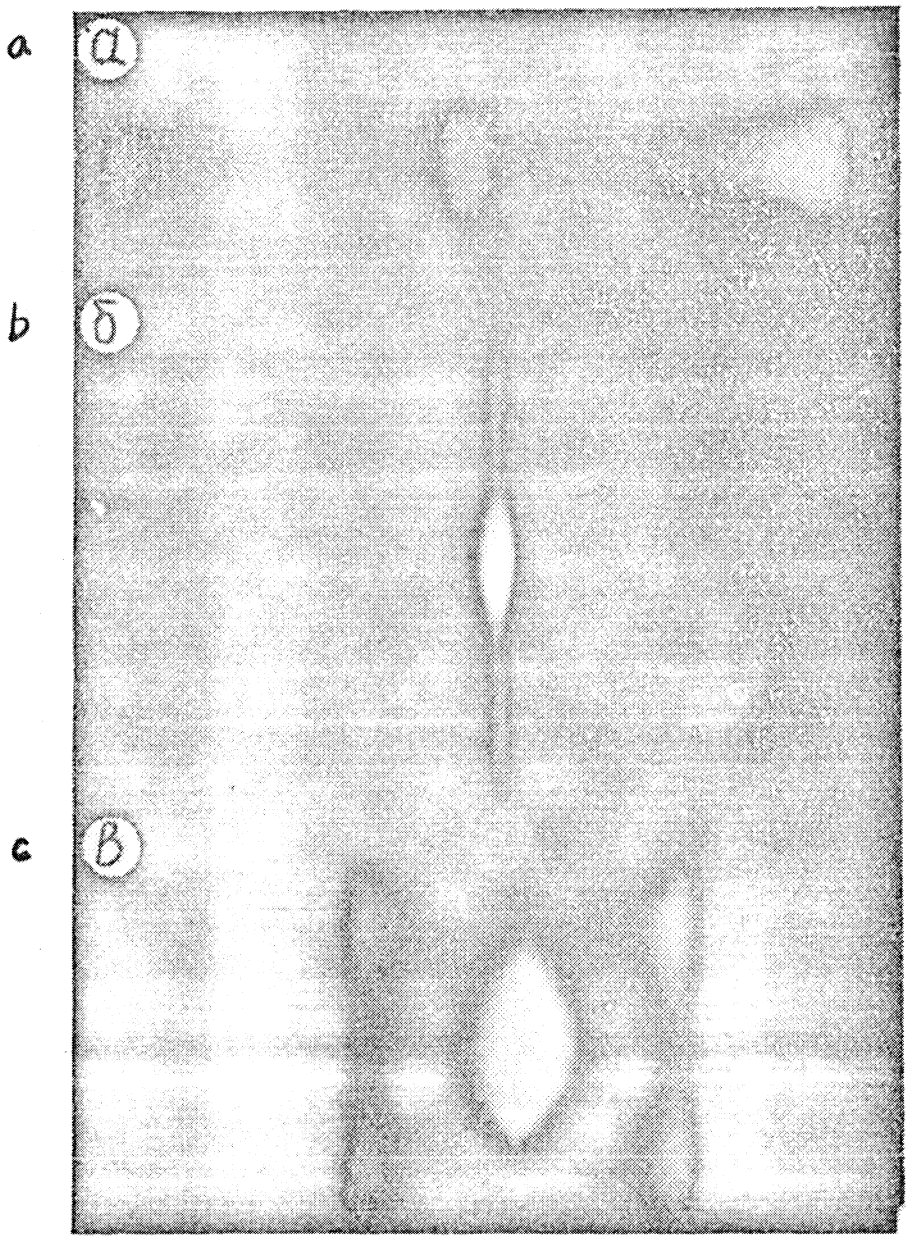

FIGURE 2: Photographs of a beam cross-section near betatron-oscillation resonances: a) vertical, b) radial, c) sum.

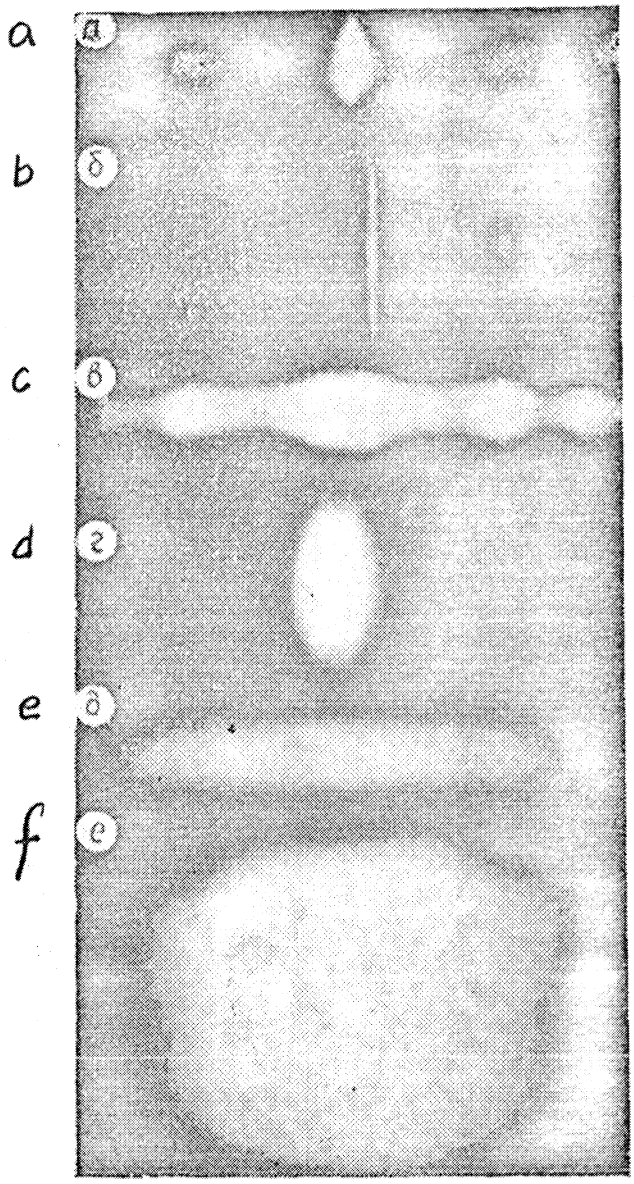

FIGURE 3: Photographs of a beam cross-section under the combined influence of two betatron-oscillation resonances: a), c) and e) two vertical; b) and f) a vertical and a radial; d) a radial and a sum.

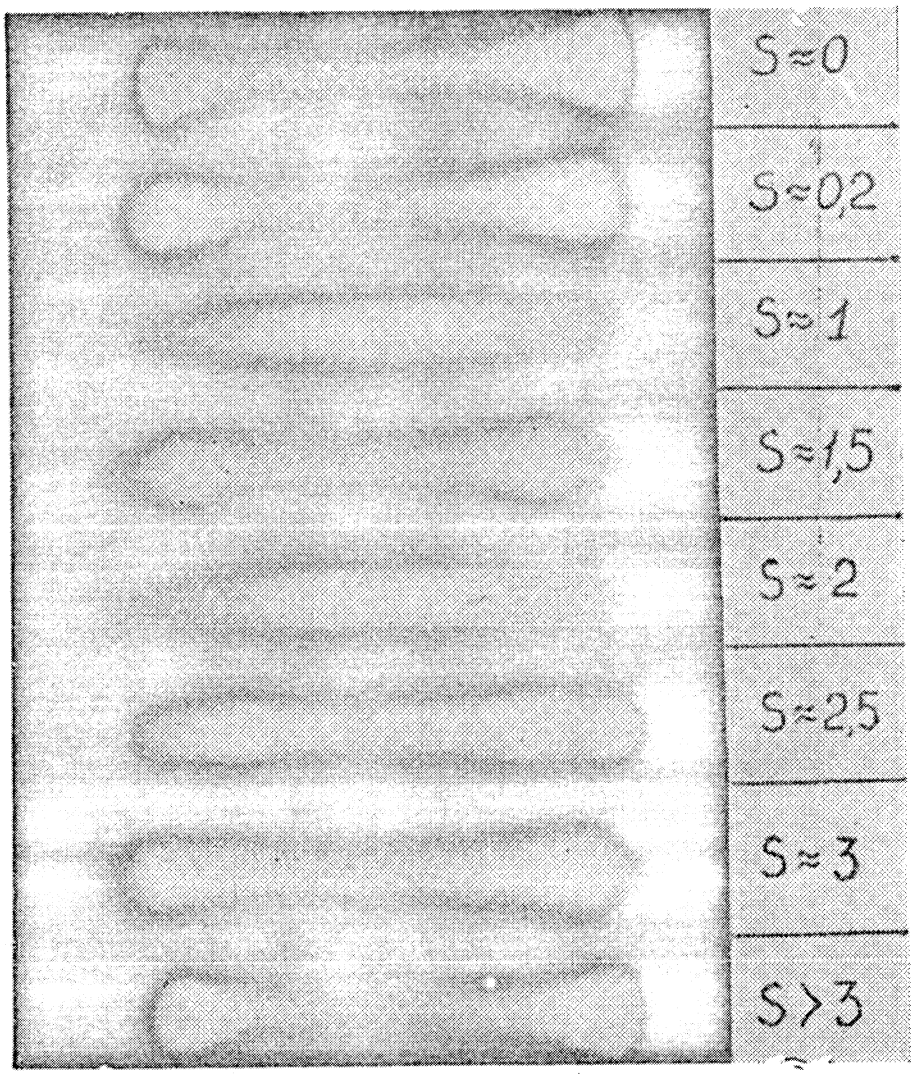

FIGURE 4: Photographs of the beam under the combined influence of two resonances of the vertical betatron oscillations as a function of the parameter s (m = 1).

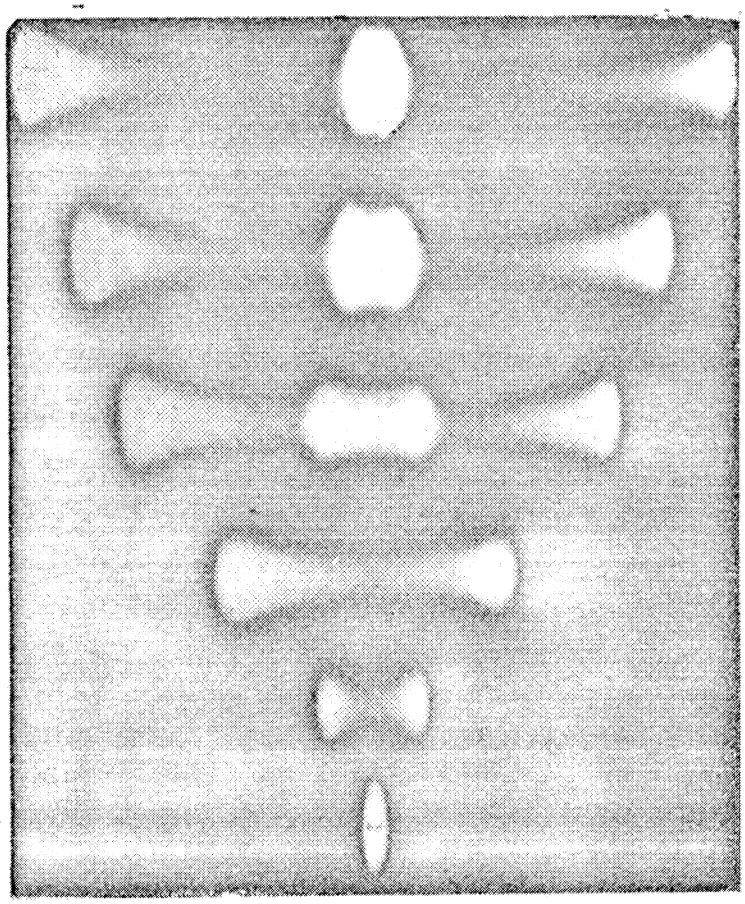

FIGURE 5: Photographs of the beam cross-section near a resonance of the vertical betatron oscillations for different frequency separations with respect to the exact resonance.

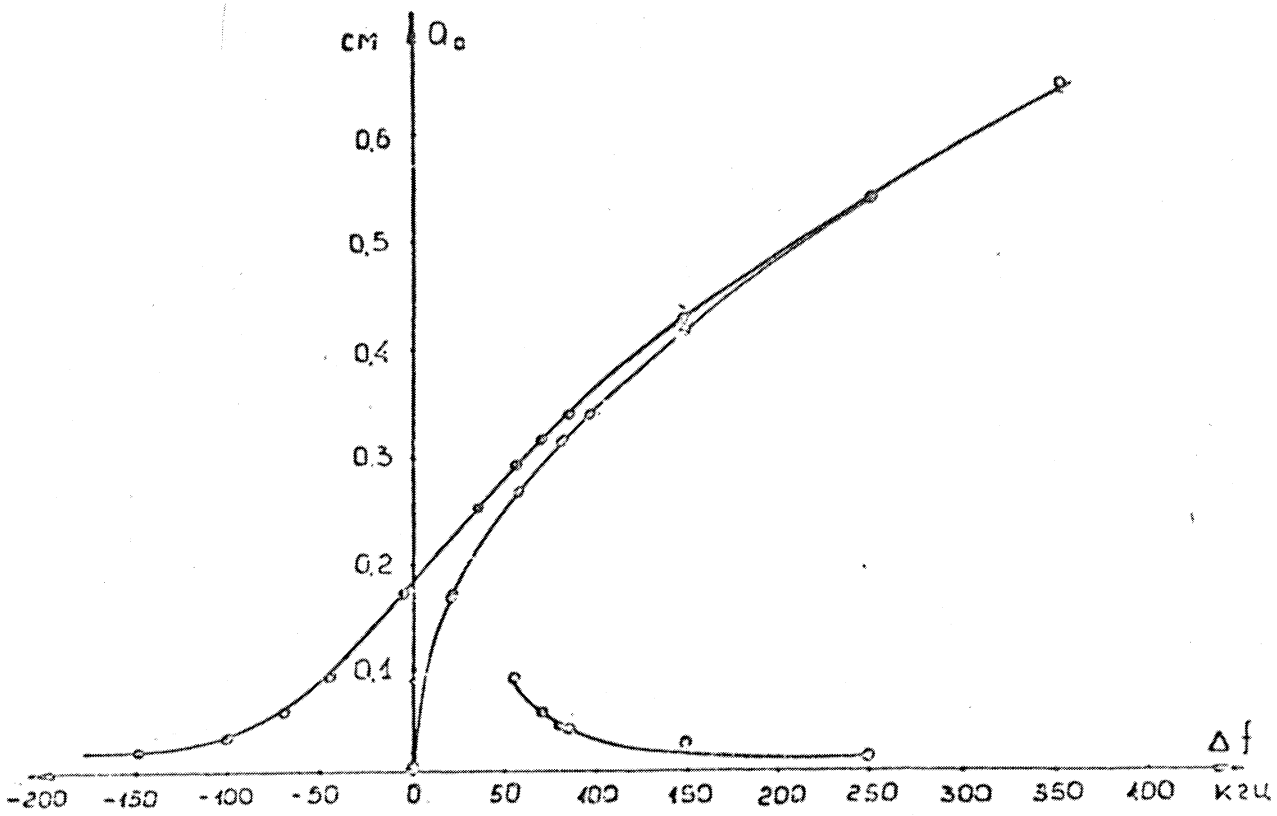

FIGURE 6: The equilibrium amplitude of the RBPS of a resonance of the vertical betatron oscillations as a function of the frequency separation. • - $U_{buildup}$ = 3 V; o - $U_{buildup}$ = 150 V. Vertical scale = cm; horizontal scale = kHz.

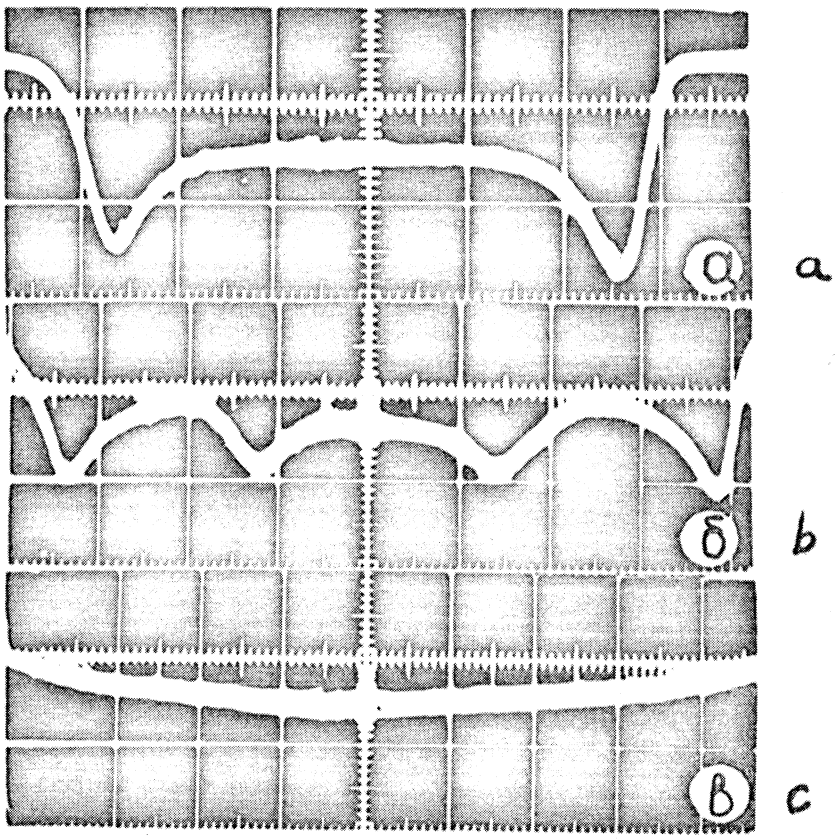

FIGURE 7: Oscillograms of the beam-density distribution with excitation of: a) a single resonance; b) two resonances $m < 0.6$; $s = 1$; c) two resonances $m = 1$; $s = 1$.

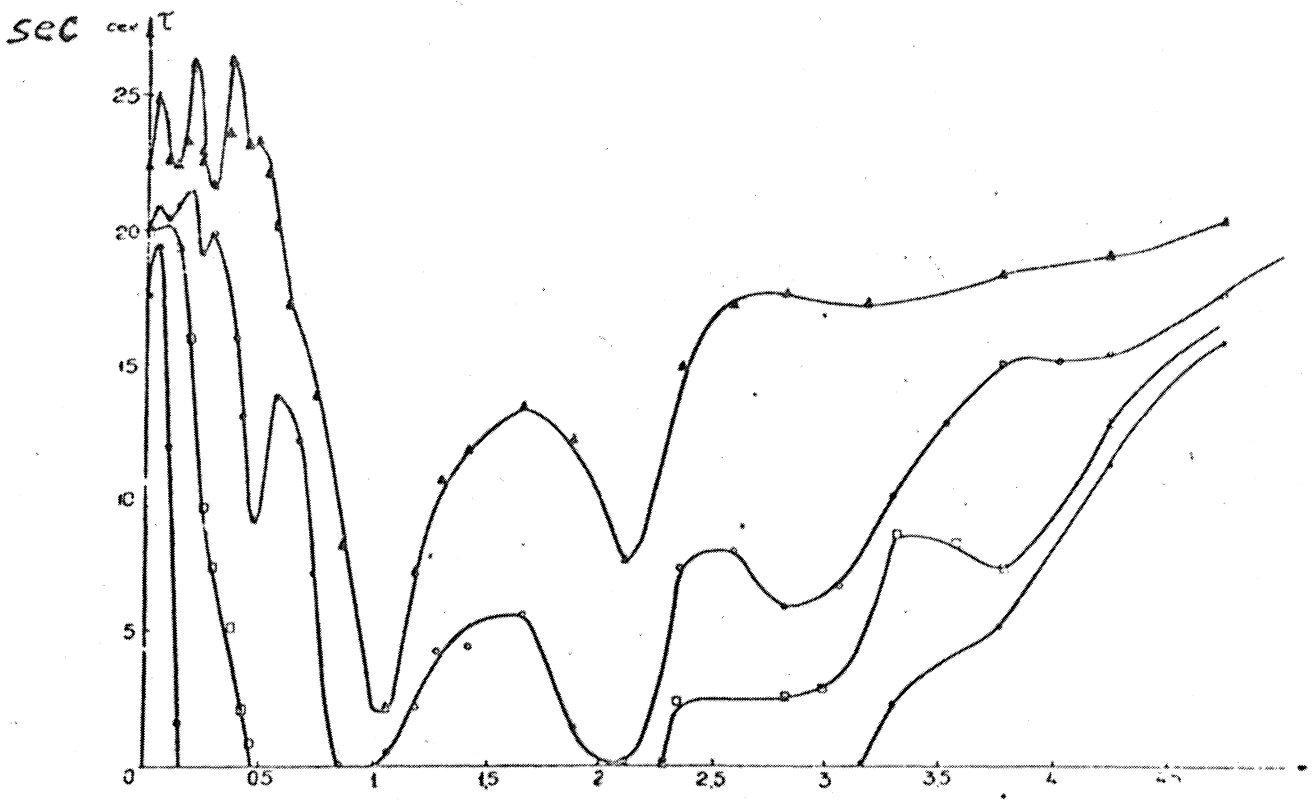

FIGURE 8: The lifetime of the particles in the RBPS as a function of the parameter s : △ - m = 0.3; o - m = 0.5; □ - m = 0.7; ● - m = 1.

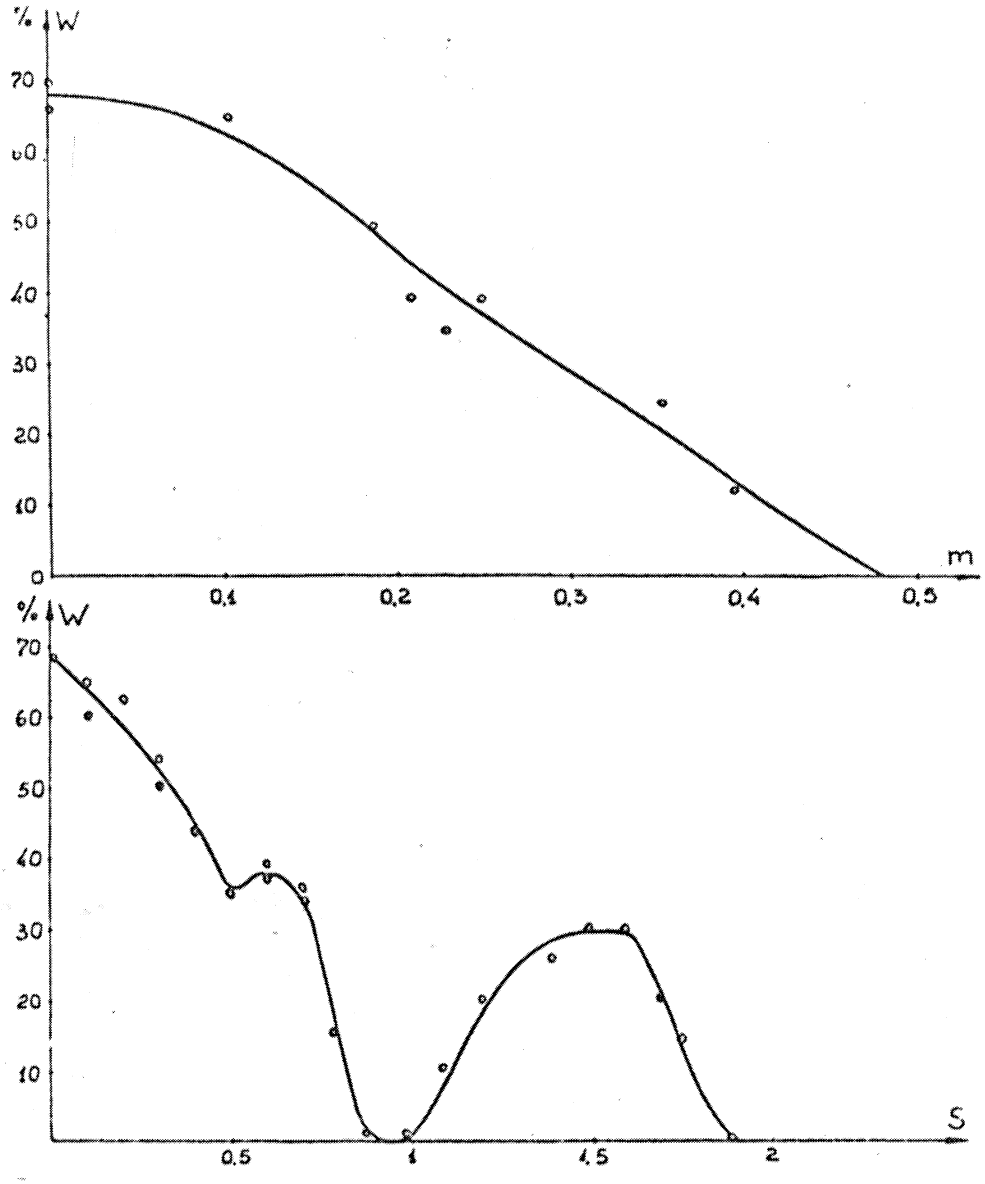

FIGURE 9: The probability of the particles' entrapment in $RBPS_1$ as a function of: a) the parameter m (s = 1); b) the parameter s (m = 0.4).

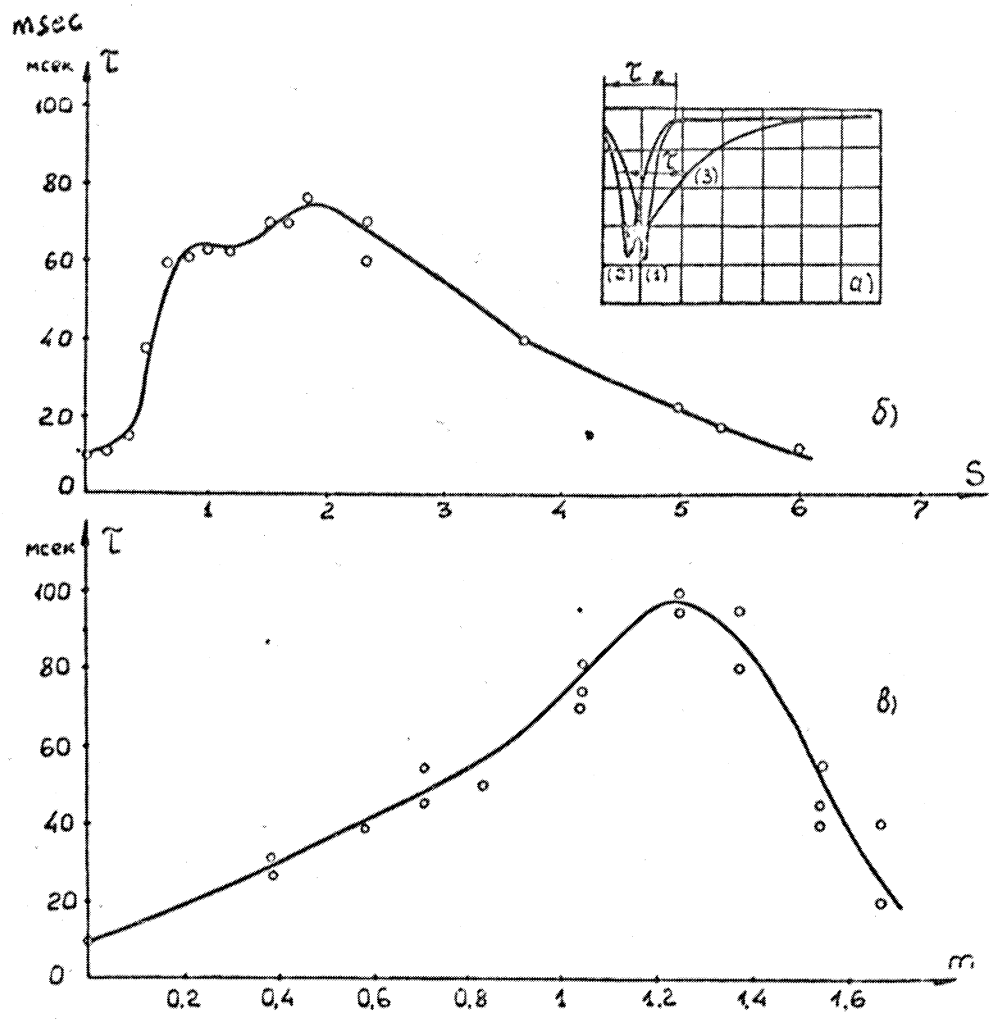

FIGURE 10: a) Oscillograms of the signal from the diaphragmed photomultiplier on passage of the beam through the amplitude region: 1- with no RBPS; 2- with one RBPS ($RBPS_1$); 3- with two RBPS.

b) Spread of the damping times as a function of the parameter s ($m \approx 1$).

c) The damping time as a function of the parameter m ($s \approx 0.6$).

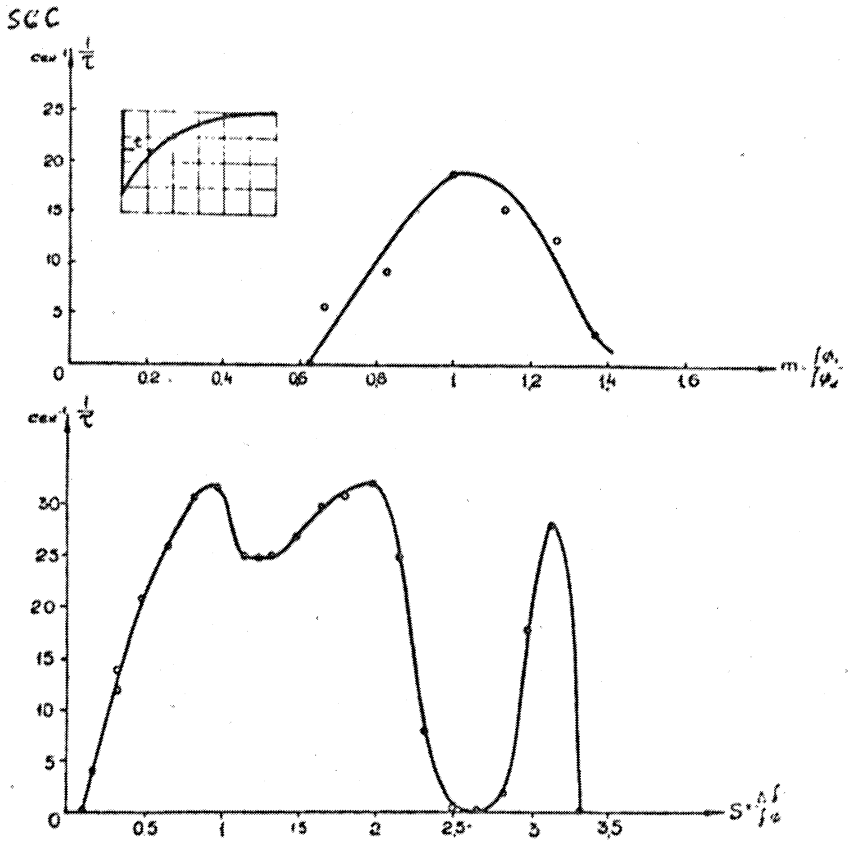

FIGURE 11: The time required for the particles to leave $RBPS_1$ when $RBPS_2$ is switched on, as a function of: a) the parameter m (s = 0.5); b) the parameter s (m = 1).

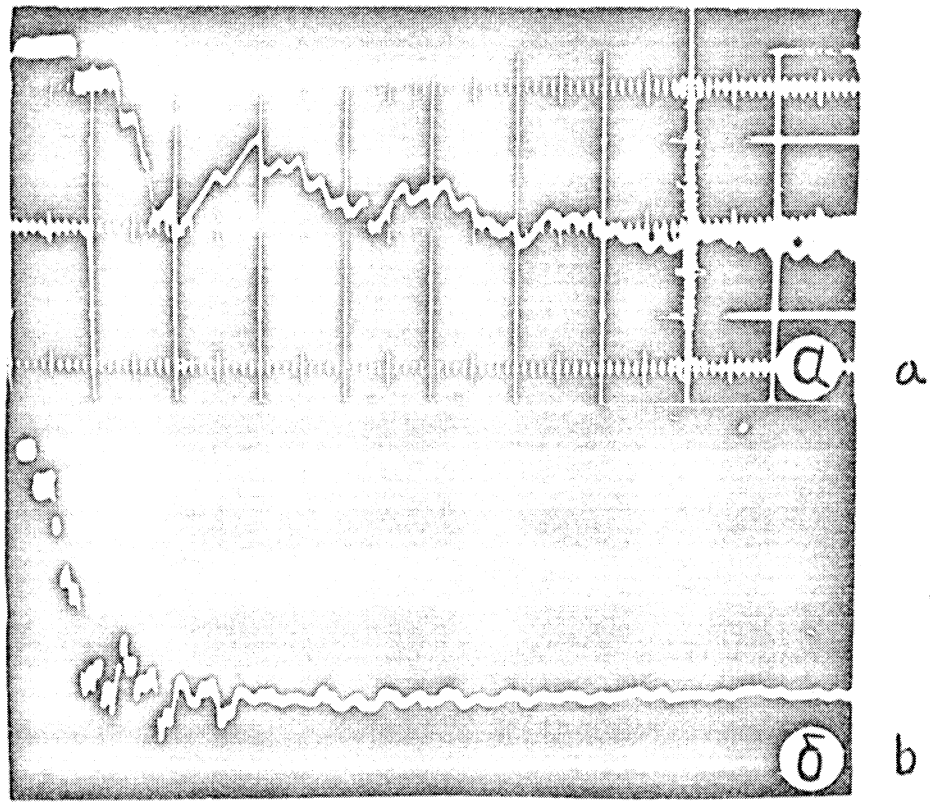

FIGURE 12: Oscillograms of the current from the diaphragmed photomultiplier (scale: 250 msec/cm).

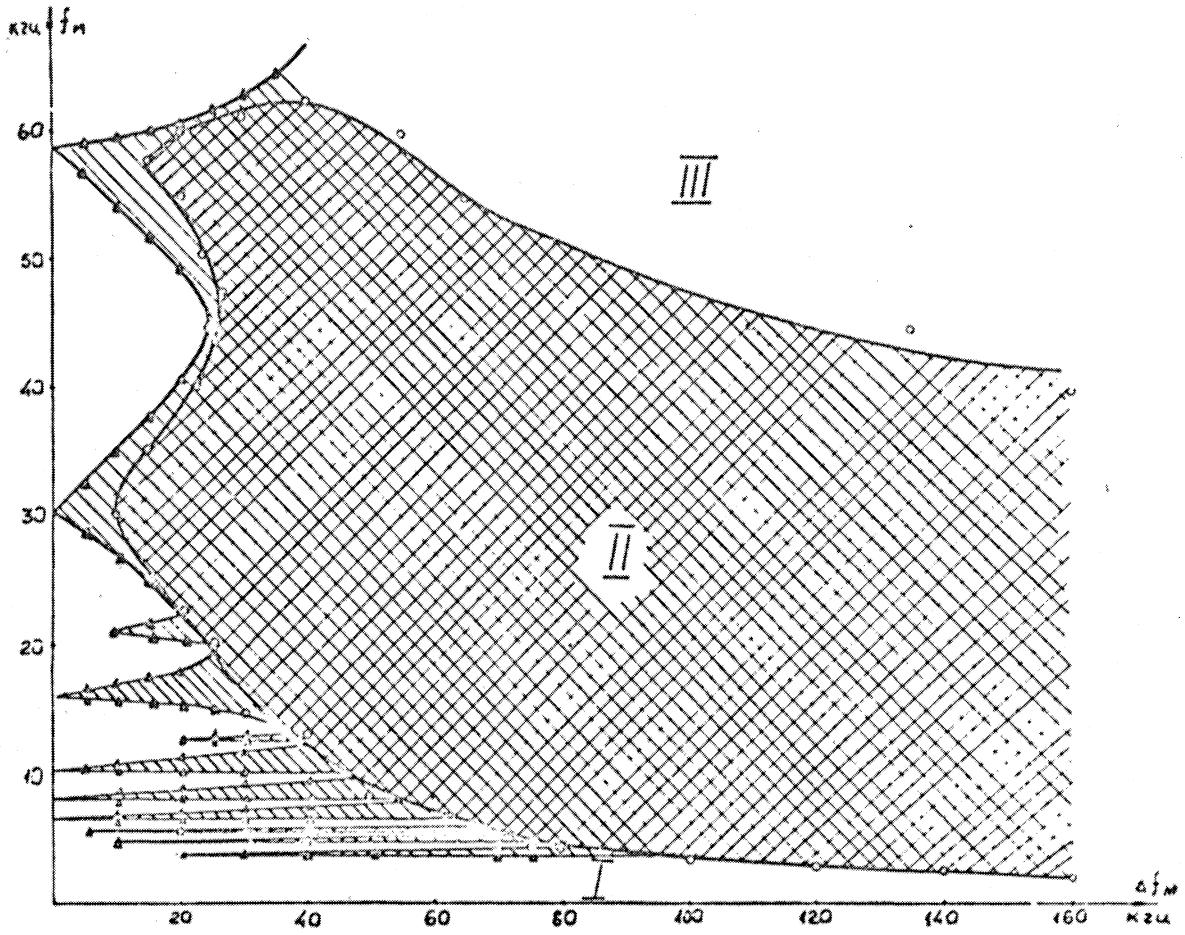

FIGURE 13: Stability diagram for periodic crossing through a resonance (f_ϕ = 36 kHz): I- slow ("adiabatic") crossing; II- stochastic region (o - complete destruction of the RBPS; Δ - partial destruction of the RBPS); III- region of "modulation" resonances. Vertical and horizontal scale = kHz.

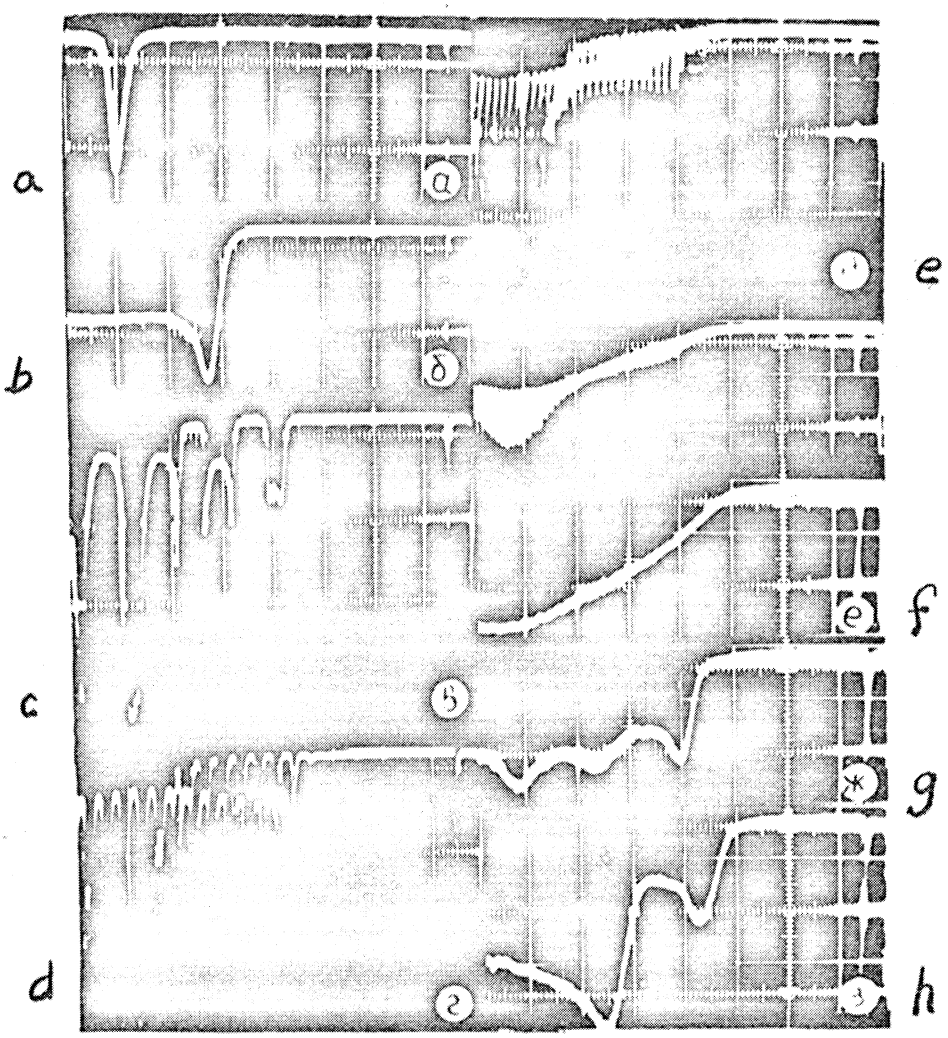

FIGURE 14: Oscillograms of the beam-density distribution characteristic of different regions: a) no resonance; b) resonance without periodic crossing; c), d) and e) transition from slow crossing to stochastic instability; f) stochastic instability; g) and h) "modulation" resonances.

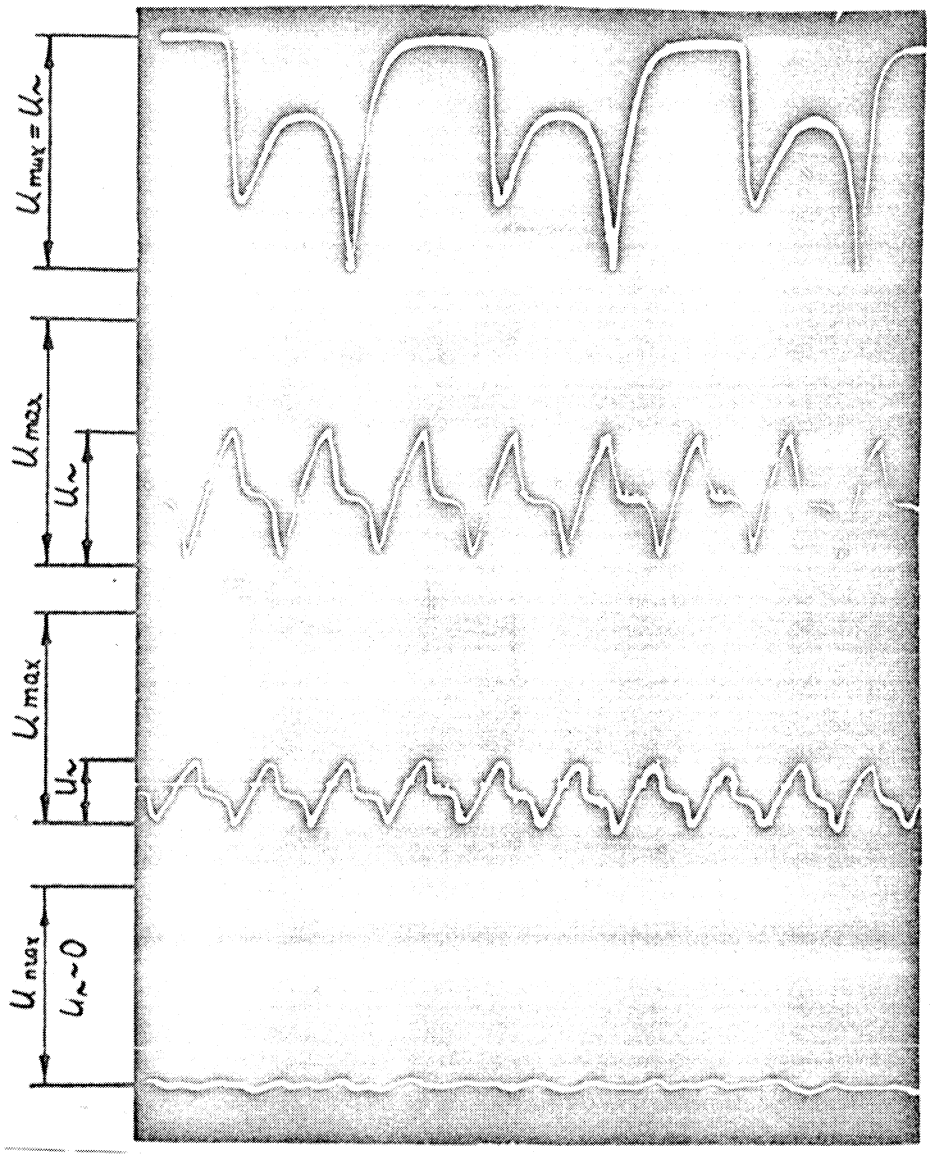

FIGURE 15: Oscillograms of the current of the diaphragmed photomultiplier in transition from an "adiabatic" crossing to the region of stochastic instability.

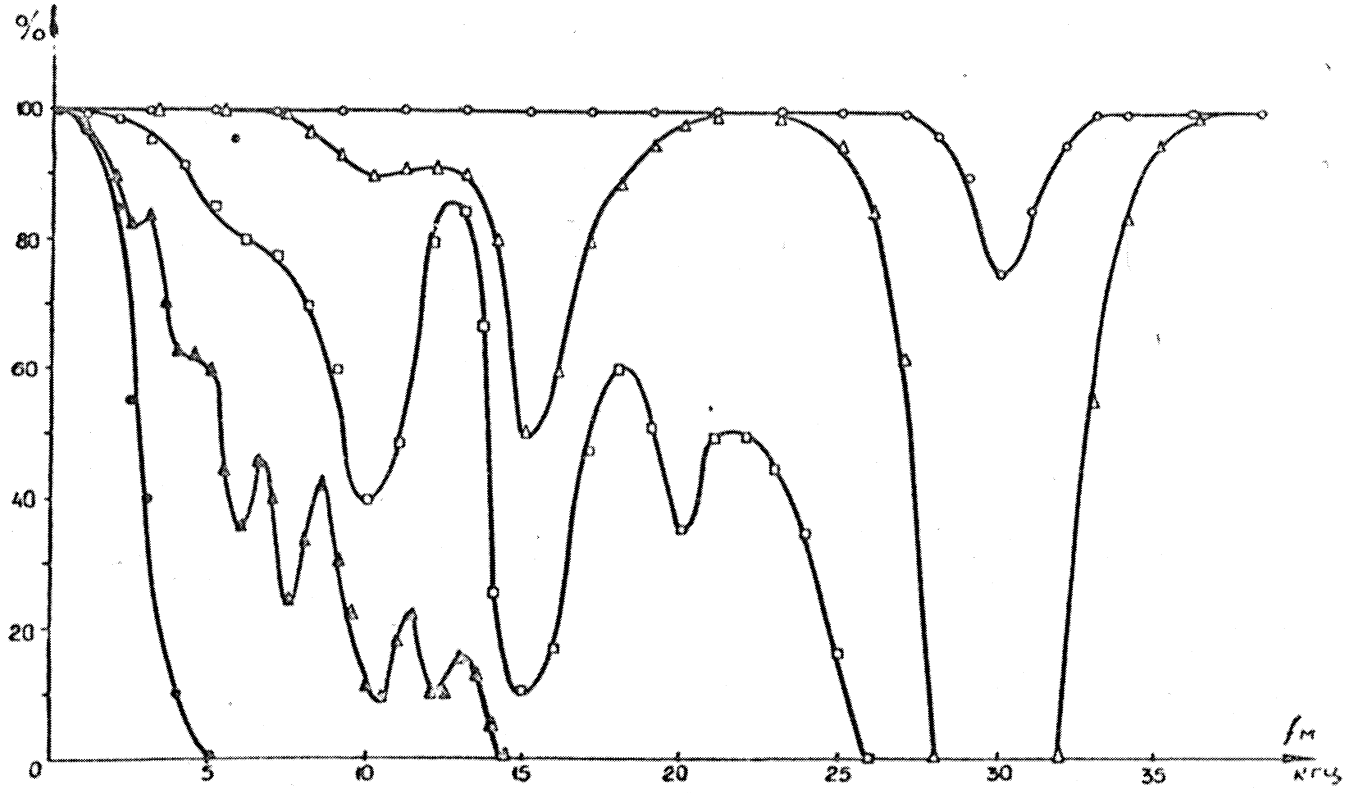

FIGURE 16: Dependence of the variable component of the photomultiplier current on the modulation frequency: o - Δf_M = 5 kHz; Δ - Δf_M = 15 kHz; □ - Δf_M = 30 kHz; ▲ - Δf_M = 60 kHz; ● - Δf_M = 120 kHz. Horizontal scale = kHz.

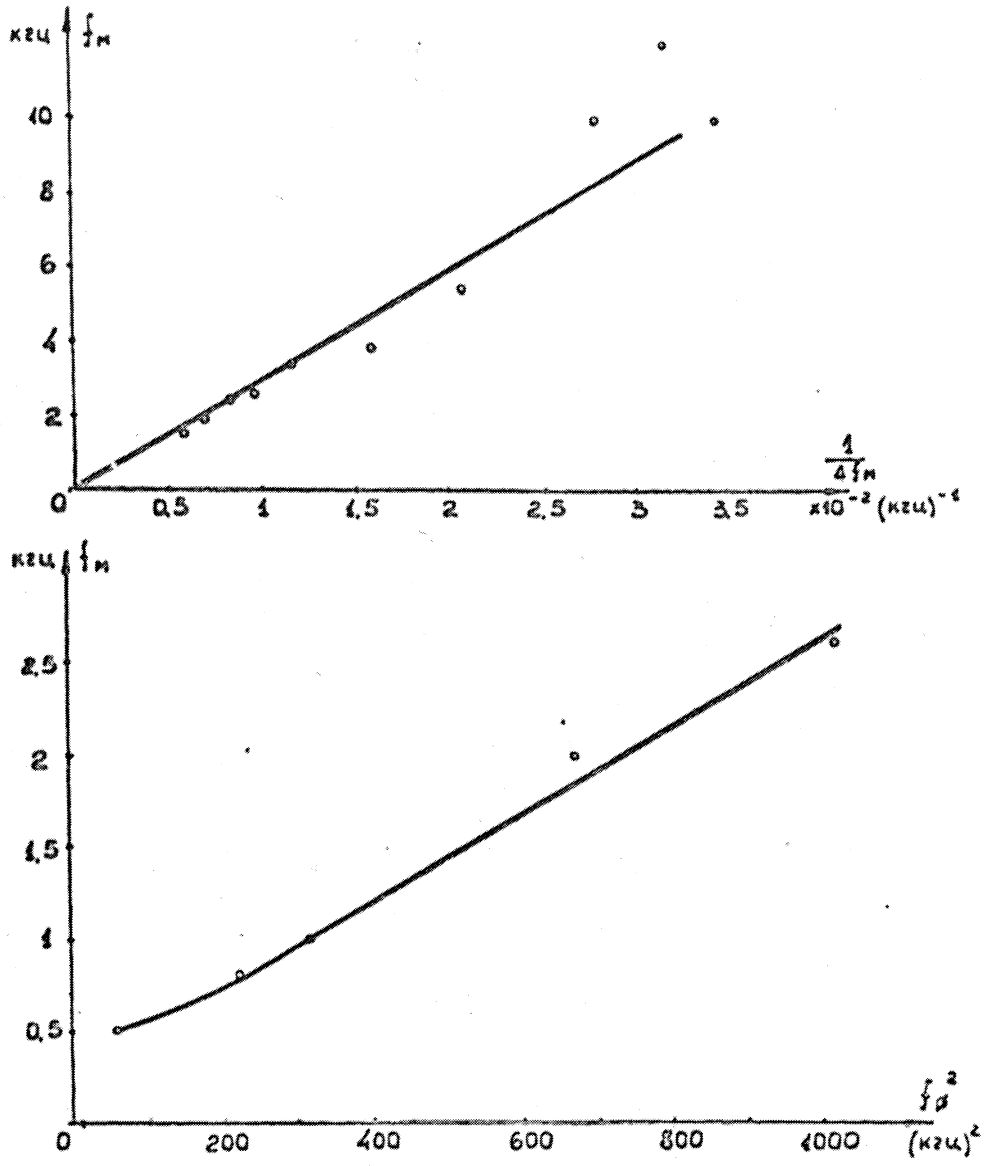

FIGURE 17: Dependence of the lower boundary of complete destruction of the RBPS on: a) the deviation (f_ϕ = 34 kHz); b) the resonance power (Δf_M = 100 kHz). Vertical scale = kHz; horizontal scale = $(kHz)^{-1}$ and $(kHz)^2$, respectively.

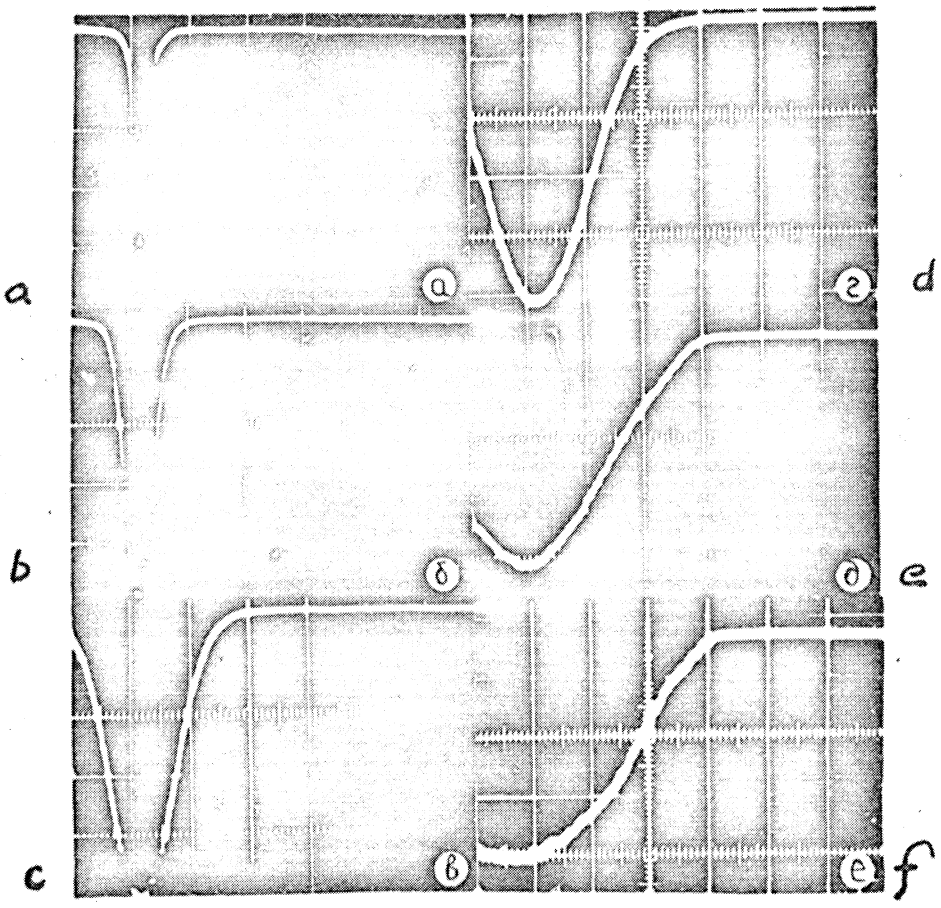

FIGURE 18: Oscillograms of the beam-density distribution in the stochastic region (f_M = 500 Hz; Δf_M = 100 kHz) as a function of f_ϕ = 0-8 kHz.

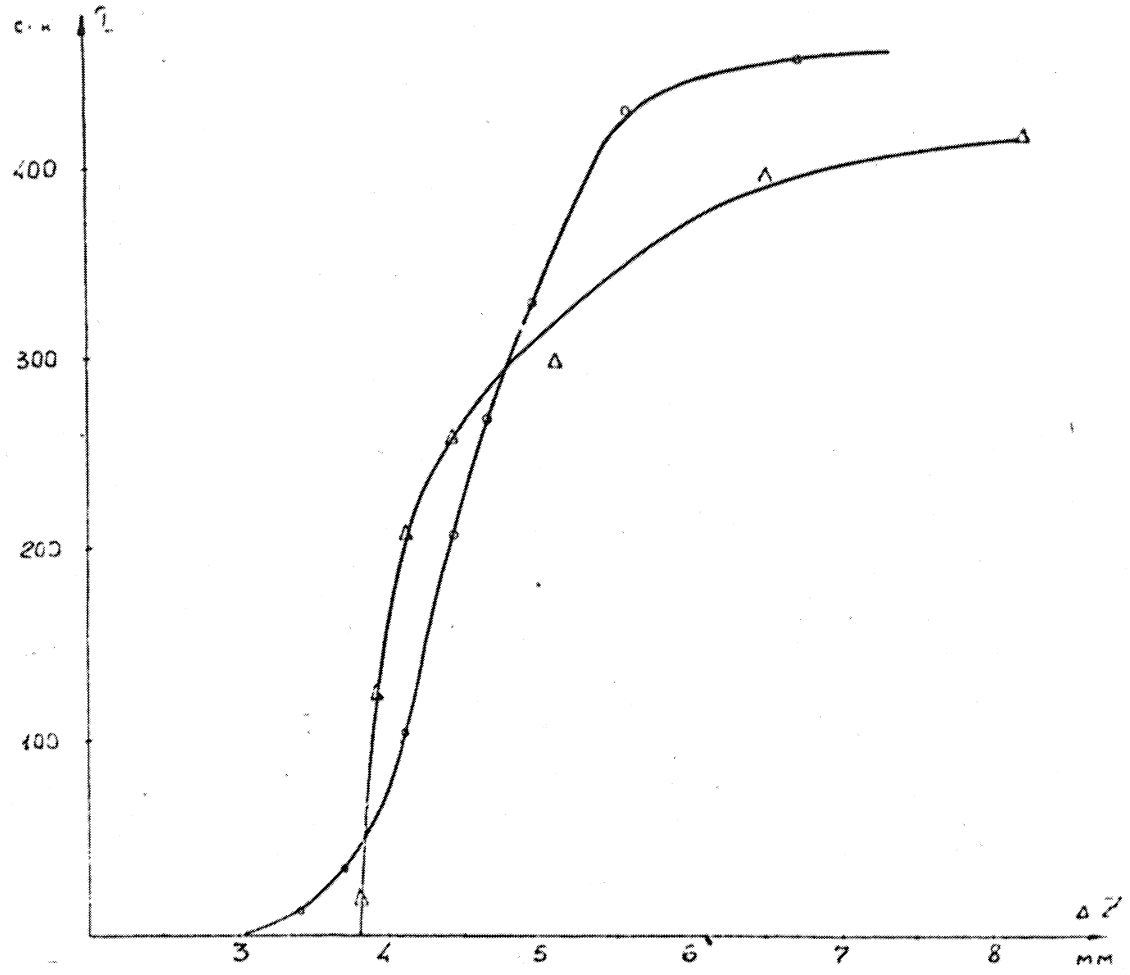

FIGURE 19: Dependence of the beam lifetime on the aperture with increasing beam size owing to: o - nonresonant buildup; Δ - stochastic instability. Vertical scale = sec; horizontal scale = mm.

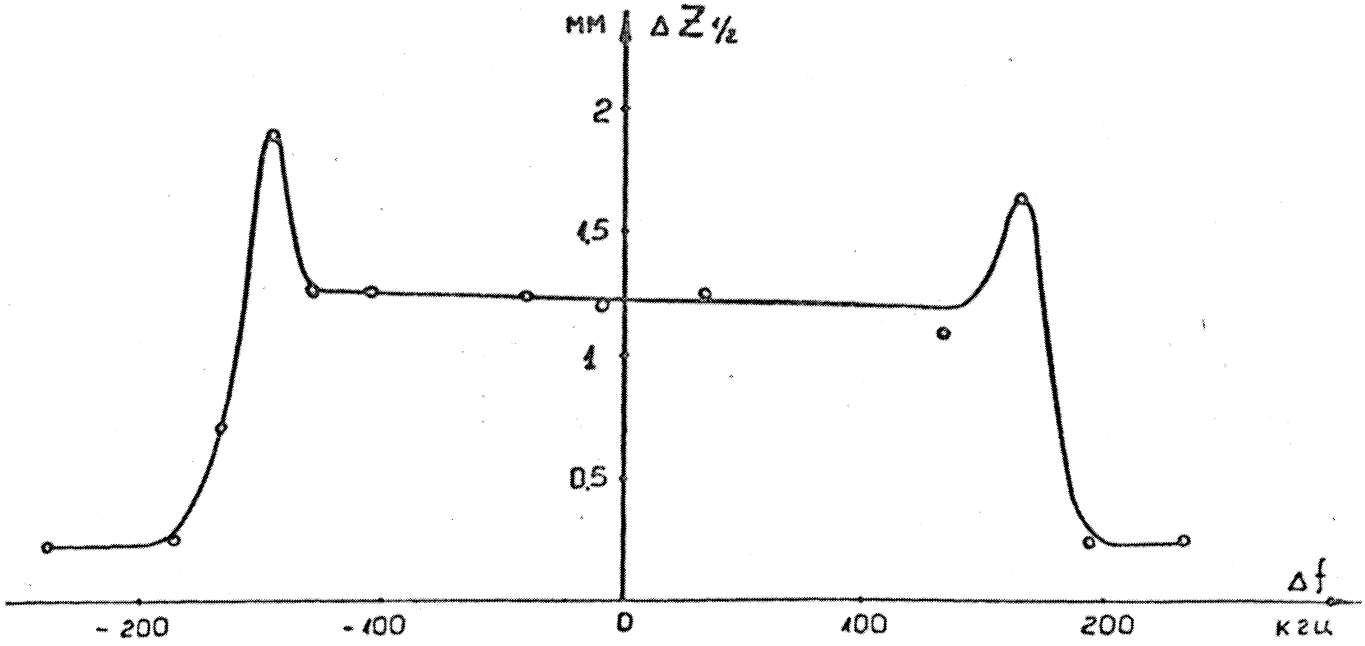

FIGURE 20: Dependence of the beam size on the buildup-frequency separation with respect to the exact resonance (f_ϕ = 7 kHz, f_M = 5 kHz, Δf_M = 200 kHz). Vertical scale = mm; horizontal scale = kHz.

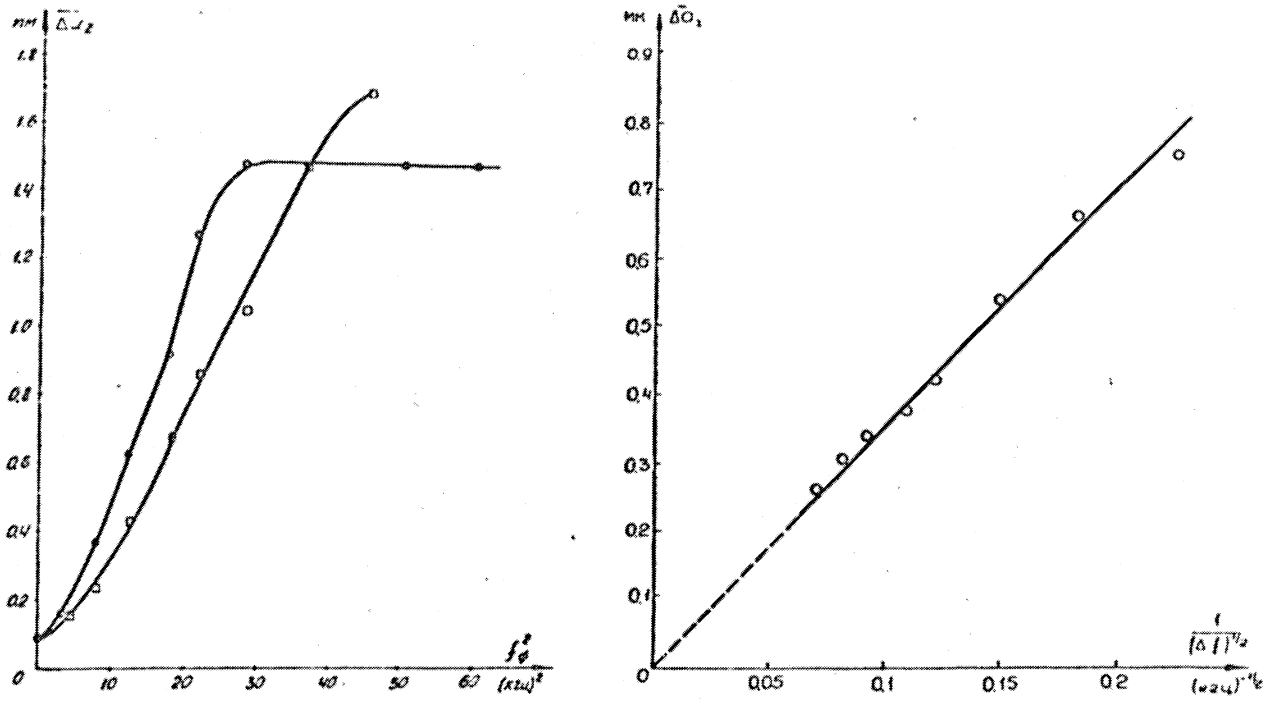

FIGURE 21: Dependence of the beam size in the stochastic region on: a) the phase-oscillation frequency in the RBPS: □ - Δf_M = 100 kHz, o - Δf_M = 30 kHz; b) the deviation (f_ϕ = 3.5 kHz). Vertical scale = mm; horizontal scale = $(\text{kHz})^2$ and $(\text{kHz})^{-\frac{1}{2}}$, respectively.

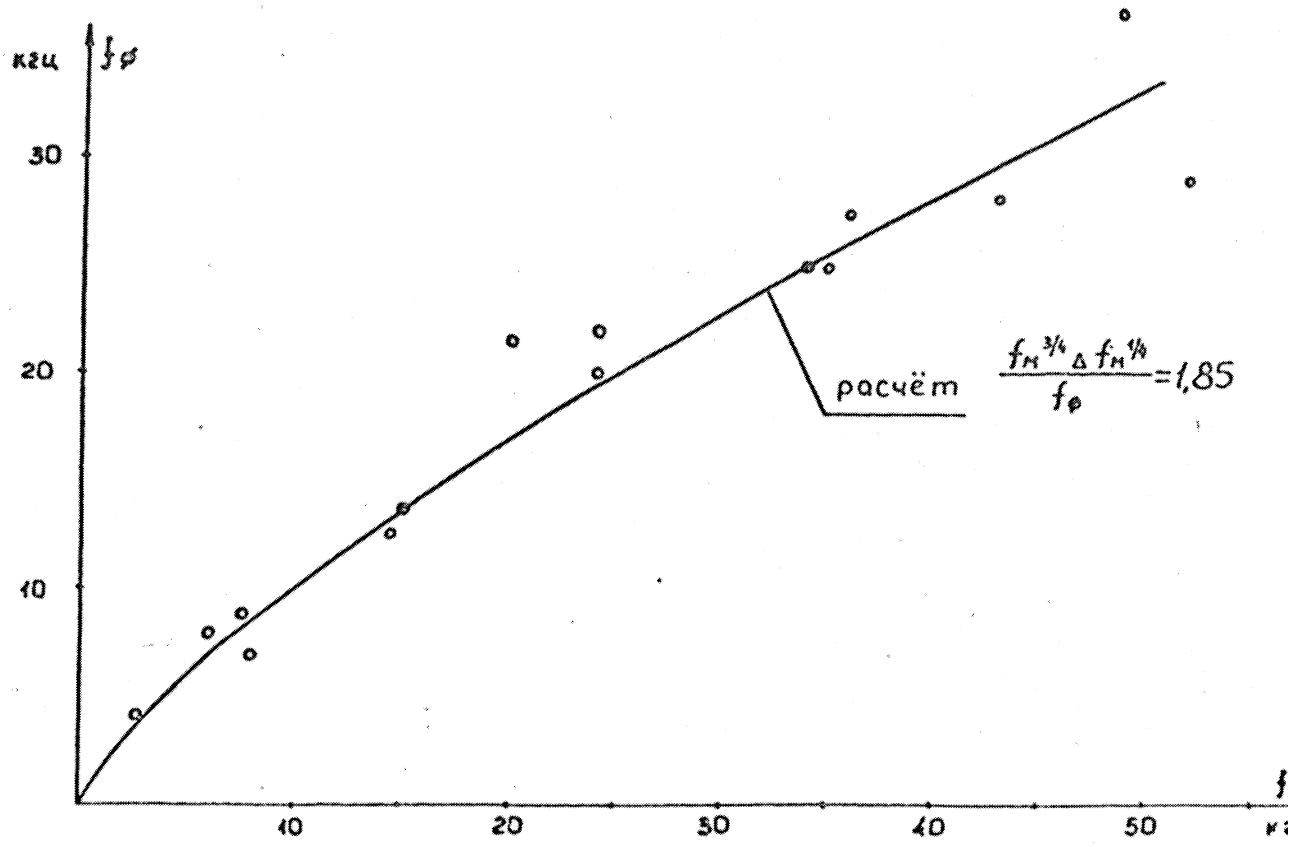

FIGURE 22: Dependence of the upper boundary of complete destruction of the RBPS on the resonance power (Δf_M = 100 kHz). Vertical scale = kHz; horizontal scale = kHz. Расчёт = calculation.